Image Cover Sheet

CLASSIFICATION	SYSTEM NUMBER
UNCLASSIFIED	154193

TITLE

ENHANCEMENTS OF THE ELASTO-OPTICS CAPABILITIES OF AVAST

System Number:

Patron Number:

Requester:

Notes:

DSIS Use only:

Deliver to:

UNLIMITED DISTRIBUTION

National Defence
Research and Development Branch

Défense nationale
Bureau de recherche et développement

DREA CR/95/461

ENHANCEMENTS of the ELASTO-ACOUSTIC CAPABILITIES of AVAST

by
D.P. Brennan

MARTEC Limited
1888 Brunswick Street, Suite 400
Halifax, Nova Scotia, Canada
B3J 3J8

CONTRACTOR REPORT

Prepared for

Defence Research Establishment Atlantic

Centre de Recherches pour la Défense Atlantique

Canada

PLEASE DIRECT ENQUIRIES TO:

THE CHIEF,
DEFENCE RESEARCH ESTABLISHMENT ATLANTIC,
P.O. BOX 1012,
DARTMOUTH, NOVA SCOTIA, CANADA
B2Y 3Z7

UNLIMITED DISTRIBUTION

National Defence
Research and Development Branch

Défense nationale
Bureau de recherche et développement

DREA CR/95/461

ENHANCEMENTS of the ELASTO-ACOUSTIC CAPABILITIES of AVAST

by
D.P. Brennan

MARTEC Limited
1888 Brunswick Street, Suite 400
Halifax, Nova Scotia, Canada
B3J 3J8

Scientific Authority
Layton E. Gilroy

April 1995

W7707-4-2846/01-OSC
Contract Number

CONTRACTOR REPORT

Prepared for

Defence Research Establishment Atlantic

Centre de Recherches pour la Défense Atlantique

Canada

ABSTRACT

The development and incorporation of the latest enhancements to the AVAST code are described. The purpose of this work was to make the modelling of the elasto-acoustic interaction more realistic, while ensuring that the code runs as efficiently as possible. To this end, several new features have been added. These include the option to use the wet modes of the structure when generating the mobility matrix, the option to generate a structural impedance matrix based upon the mass, damping and stiffness matrices, the implementation of a multi-frequency boundary integral equation method, decomposition of the current AVAST program modules in order to allow for restart analyses, implementation of a convergence acceleration technique for use in the calculation of the waveguide Green's function, incorporation of the hypersingular Burton and Millar boundary integral equation method and the implementation of a coupling between the fluid and structural models for the transient case.

Résumé

Cette étude, qui décrit le développement et l'incorporation des derniers perfectionnements du programme AVAST, avait pour but de rendre encore plus réaliste la modélisation de l'interaction élasto-acoustique, tout en assurant des passages de programme aussi efficaces que possible. Plusieurs caractérisques nouvelles ont été ajoutées à cette fin, dont l'option d'utilisation des modes immergés de la structure pour la production d'une matrice d'impédance structurale basée sur les matrices de masse, d'amortissement et de rigidité et la mise en oeuvre d'une méthode d'équation intégrale aux limites multi-fréquences, la décomposition des modules actuels du programme AVAST pour permettre les analyses du redémarrage, la mise en oeuvre d'une technique de calcul pour convergence accéléré de la fonction de Green des guides d'ondes, l'incorporation de la méthode d'équation intégrale aux limites hypersingulière de Burton et Millar et la mise en oeuvre d'un couplage entre le modèle fluide et le modèle structural pour le cas transitoire.

TABLE OF CONTENTS

TABLE OF CONTENTS - Continued

LIST OF TABLES

LIST OF FIGURES

1. INTRODUCTION

Phase I, II and III of the Martec/DREA collaborative investigation in underwater acoustics has resulted in the development of a series of computer programs, collectively named AVAST, for the numerical prediction of the acoustic radiation and scattering from submerged elastic structures immersed in either finite depth, half-space or infinite fluid domains. AVAST combines both the finite element method for the structure and the boundary integral equation technique for the surrounding fluid. The finite element method is used to define a mechanical mobility matrix relating excitation forces to structural velocities along the fluid/structure interface. The boundary integral equation method is used to generate a system of equations relating surface velocities to fluid acoustic pressures.

In an attempt to improve the modelling of sound radiated and/or scattered from submerged structures, several enhancements have recently been incorporated into the previously existing AVAST suite. These include the option to use the wet modes of the structure when generating the mobility matrix, the option to generate a structural impedance matrix based upon the mass, damping and stiffness matrices, the implementation of a multi-frequency boundary integral equation method, decomposition of the current AVAST program modules in order to allow for restart analyses, implementation of a convergence acceleration technique for use in the calculation of the waveguide Green's function, incorporation of the hypersingular Burton and Millar boundary integral equation method and the implementation of a coupling between the fluid and structural models for the transient case.

In the discussion which follows, details concerning the development and incorporation of these latest enhancements to the AVAST suite will be presented. In addition, a state of the art literature review on infinite wave envelope elements and a summary of an investigation into the sound radiated from partially submerged, point excited bodies, will also be presented.

2. RESTRUCTURING THE AVAST CODE

2.1 Introduction

In the original version of the AVAST suite, all relevant input data, including both the geometry of the radiating body and the position of the exterior field points, had to be supplied by the user at the start of an analysis. Once this information was collected, the program would then proceed with the generation of the associated numerical model of the coupled fluid/structure system, which included the formulation of frequency dependent fluid matrices, the generation of a mechanical impedance (or mobility) matrix, the coupling of the fluid and the structural equations, solution of the wet surface velocity and acoustic pressure fields and finally, the solution of exterior field pressures. One major drawback with a program structure of this type is the penalty paid by the user when pressures at additional field locations are required. In such an event the entire analysis would have to be re-run, representing the unnecessary duplication of recalculating surface pressures and velocities.

In light of this shortcoming in the structure of the AVAST suite, a new modular version of the code was developed. With this new program format intermediate results can now be saved and reused, representing potential savings in analysis time.

2.2 Modular Code Structure

The original AVAST code has now been decomposed into seven distinct program modules: FLUMOD, INWAVE, UNCOUP, MOBIL, COUPLE, PVSURF and EXTFLD. The user may execute any or all modules by responding positively to a prompt offered by the main driver program. A description of the function and data requirements for each program module is provided in separate sections below.

2.2

2.2.1 FLUMOD Program Module

The FLUMOD module generates the H and G matrices which represent the numerical model of the acoustic fluid medium [1]. In terms of input data requirements, the user must supply data related to the physical properties of the fluid, including:

- The number of structural bodies immersed in the fluid;
- Bem file prefixes (the bem file contains the geometry of the structural wet surface);
- The number of integration points used when generating the H and G coefficient matrices;
- The fluid sound speed and density;
- The forcing frequency; and
- The type of fluid domain under consideration (i.e., full space, half space, or waveguide domains).

Once all the above information has been entered, the program proceeds to generate the H and G coefficient matrices, storing this information on a binary data file having the extension **hgm**. In addition, a second data file (having extension **geo**) is also generated by FLUMOD module. This file contains data related to the geometric properties of the fluid model and is used by several other AVAST program modules.

2.2.2 INWAVE Program Module

The INWAVE module generates the incident pressure terms used in acoustic scattering analyses. If selected by the user, INWAVE searches the working directory for the appropriate **geo** file generated by a previous run of the FLUMOD module. Once the surface panel geometry is read in, INWAVE then searches the working directory for a file having the extension **src** and sharing the same file name prefix as that used by the **geo** file. If this file exists, INWAVE opens it and extracts the number (up to a maximum of 200) and location of acoustic sources. The program then calculates the incident pressure values on the surface of the structure and stores these values on a binary data file having the extension **inw**.

2.2.3 UNCOUP Program Module

The UNCOUP module allows the user to solve for the wet-surface acoustic pressures provided that the user supplies either surface normal displacements, incident pressure values, or both. Upon execution, the program prompts the user for the type of analysis to be performed, i.e., radiation, scattering or combined radiation and scattering. If an acoustic radiation analysis is to be performed (either with or without scattering), the program will search the working directory for a data file having the extension **sgd**. This file contains the wet surface displacements which are used to calculate a set of surface acoustic pressures. If an acoustic scattering analysis is to be performed (either with or without radiation) UNCOUP then searches for the **inw** file, (generated during a previous run of INWAVE module), which contains the incident source terms. These incident pressure values are then read in by the program and combined, if necessary, with the radiation terms. Once the surface acoustic pressures have been generated, UNCOUP writes these values to an output file having the extension **prs**. These surface pressure terms can then be used, in combination with the normal displacements and incident pressure terms, to generate exterior field pressures.

2.2.4 MOBIL Program Module

The MOBIL program module generates the structural mobility matrix required for coupled fluid/structure interaction problems. If selected by the user, MOBIL first searches the working directory for the appropriate VAST [2] compatible **t48** and **t49** files, which store the structural stiffness and mass matrices, respectively. If these files are available, MOBIL then prompts the user for Rayleigh damping coefficients (used to generate the structural damping matrix). MOBIL then combines the structural mass, stiffness and damping matrices (along with the driving frequency found on the **geo** file) to form the structural impedance matrix, which is then inverted in order to generate the structural mobility matrix. The structural mobility matrix is then stored on a binary data file having extension **mbl**.

2.2.5 COUPLE Program Module

The COUPLE module combines the structural mobility matrix (stored in the **mbl** file) with the fluid H and G matrices (stored in the **hgm** file) to form a single system of equations which relate fluid acoustic pressures to structural and fluid loads. Once generated, this coupled system of equations is then stored on a binary data file having the extension **fsm**.

2.2.6 PVSURF Program Module

The PVSURF module extracts the coupled system of equations, stored in the **fsm** file, and solves for the wet surface acoustic pressures, surface displacements and surface normal velocities. The pressures, displacements and velocities are then stored on output data files having the extensions **prs**, **trn** and **nrm**, respectively.

2.2.7 EXTFLD Program Module

The EXTFLD module generates exterior field pressures, provided that surface acoustic pressures and normal velocities have been computed during a previous run of the PVSURF module. Initially, EXTFLD searches the working directory for the data files **prs** (containing the surface pressures), **nrm** (containing the surface normal velocities) and **efp** (containing the number and location of a series of exterior field points). If all three files are available EXTFLD will then proceed with the calculation of the exterior field acoustic pressures. Once this step has been completed the EXTFLD module then writes these exterior pressures to an output data file having the extension **fpr**.

3. RISC-BASED VERSION OF THE AVAST SUITE

A recent review of DREA's computing requirements has resulted in the decision to replace the aging VAX 6420 VMS mainframe cluster with a number of RISC-based workstations. As a result, much of the code now resident on the mainframe cluster, including both the VAST and AVAST suites, must now be ported to these new platforms.

The installation of the AVAST code on the node RAINBOW proceeded without any difficulty. Previous experience gained while preparing RISC-based versions of the code for the HP-720 computer allowed Martec staff to generate an executable version of the code on RAINBOW relatively quickly. The source code was transferred from the VAX 6420 to the RAINBOW via the FTP file transfer facility, where it was compiled using the compiler switches -c and -static.

4. STRUCTURAL IMPEDANCE MATRIX

4.1 Introduction

In the original version of the AVAST suite, the modal characteristics of the dry structure were used to establish a mobility matrix, M, relating surface nodal velocities, v, to applied structural loads, f:

$$\{v\} = [M]\ \{f\} \tag{4.1}$$

Unfortunately, for driving frequencies below the first natural frequency of the dry structure, the modal mobility approach failed to yield acceptable results [3]. Experience has shown that when the structure is excited at frequencies corresponding to the first few "wet" natural modes of the structure (which are always lower than the first dry mode) the response generated by the mobility approach appears to be essentially static.

Since the structural response at the first few natural frequencies is generally of significant interest, a new structural impedance modelling methodology was recently proposed [4] and has now been implemented in the latest version of the AVAST code. The impedance modelling approach provides the user with the option of generating a structural impedance matrix, Z_s, based upon the structural mass (M_s), damping (C_s) and stiffness (K_s) matrices.

$$[Z_s] = [K_s] + i\omega[C_s] - \omega^2[M_s] \tag{4.2}$$

where ω represents the driving frequencies in radians per second.

In the following sections, a review of the impedance matrix modelling methodology is presented. This is followed by a numerical example involving acoustic radiation from a uniformly driven pulsating sphere submerged in sea water.

4.2 Modelling Radiated Noise Using the Impedance Matrix Approach

For the analysis of time harmonic acoustic radiation, AVAST uses VAST [2] as a basis to establish a finite element model of the structure. AVAST combines the assembled structural stiffness, damping and mass matrices to form a structural impedance matrix in the form given above in Equation (4.1). In this form, the impedance matrix provides a relationship between structural displacements, x, fluid pressures, p, and applied structural loads, f,

$$[Z_s]\{x\} = [L]\{p\} + \{f\} \tag{4.3}$$

where the matrix [L] provides a transformation between surface pressure at the fluid/structure interface and structural loads [5].

The AVAST formulation for the acoustic fluid is based upon the Helmholtz integral relationships [6]. The scalar wave equation for the acoustic medium is replaced by an integral equation over the wetted surface (Γ) of the structure, which in turn is approximated by a system of algebraic equations,

$$[A]\{p\} = \rho\omega^2[B]\{x_n\} + \{\phi_i\} \tag{4.4}$$

where ρ represents the fluid density, ω is the angular frequency, $\{p\}$ and $\{x_n\}$ are column vectors whose n-th components are the pressure and normal displacement on the n-th subdivision Γ_n of Γ and $\{\phi_i\}$ is a column vector whose n-th component is a function of the incident pressure at a point on Γ_n.

In a pure radiation problem the incident pressure vanishes and coupling of the governing structural and fluid equations leads to a partitioned system for displacement (x) and pressure (p),

$$\begin{bmatrix} Z_s & -L \\ -\rho\omega^2 BH & A \end{bmatrix} \begin{Bmatrix} x \\ p \end{Bmatrix} = \begin{Bmatrix} f \\ 0 \end{Bmatrix} \tag{4.5}$$

where the matrix [H] provides a transformation between surface normal and global displacements.

Direct solution of Equation (4.4) is, unfortunately, prohibitively expensive for models of any significant size. However, by eliminating the structural displacements, x, Equation (4.4) can be reduced to a single combined matrix equation of the form,

$$([A] + [R][L])\{p\} = [R]\{f\} \tag{4.6}$$

where

$$[R] = -\rho\omega^2[B][H][Z]^{-1} \tag{4.7}$$

Once the fluid acoustic pressures have been computed they may then be combined with the wet surface structural displacements (generated via Equation 4.2) to yield acoustic field pressures via the exterior Helmholtz equation [1,2,5,6].

4.3 Numerical Example

Verification of the structural impedance modelling feature was carried out by comparing results produced by AVAST with solutions reported in the literature [7]. One such case involved the acoustic radiation from a thin-walled spherical shell submerged in water and driven internally with a spherically symmetric (uniform), time harmonic pressure load. Since the solution is also spherically symmetric, the field solution depends only on the radial distance from the sphere centre. The physical properties of both the sphere and surrounding fluid are provided in Table 4.1.

By adopting symmetry boundary conditions, the structural model was limited to only a single octant of the sphere. A total of 96 four-noded structural shell elements and 192 triangular fluid panel elements were used to model the structural and fluid domains, respectively. The numerical model was used in a series of trial which involved a number of drive frequencies. Figure 4.1 provides a comparison of the AVAST and the corresponding analytical results.

4.4

TABLE 4.1: Physical Properties	
Sphere radius	1.0 m
Shell thickness	0.05 m
Young's modulus	2.07 x 10" Pa
Poisson's ratio	0.3
Shell material density	7669 kg/m^3
Fluid density	1000 kg/m^3
Fluid sound speed	1524 m/s
Internal pressure	1.0 Pa

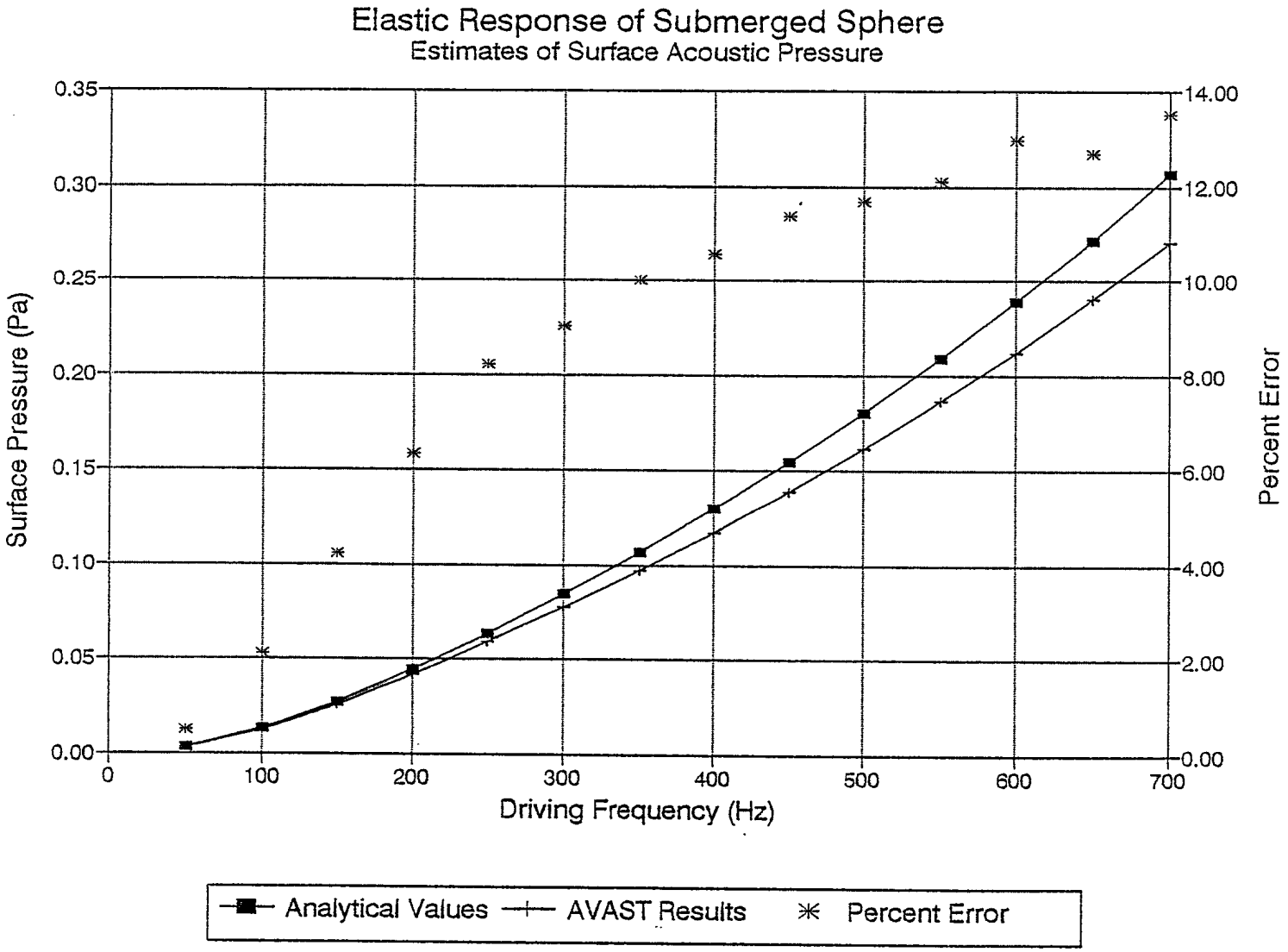

FIGURE 4.1: Elastic Response of Submerged Sphere

5. CONVERGENCE ACCELERATION FOR THE CALCULATION OF THE WAVEGUIDE GREEN'S FUNCTION

5.1 Introduction

The boundary element method (BEM) has been an efficient numerical technique for the modelling of acoustic radiation and scattering from bodies of arbitrary shape immersed in homogeneous free space or half space fluid domains [8]. For a free space problem, the Green's function used in the BEM formulation is simply the point source solution. For a half space problem with a perfectly reflecting plane, the Green's function can be obtained by supplementing the free space form with an image point source [8,10].

When the acoustic domain is bounded by two reflecting planes (i.e., waveguide) the Green's function can no longer be expressed in closed form and must be represented as the sum of an infinite number of terms. For simplicity, each term may be considered as a separate reflected image of full space Green's function.

Although the concept of this type of image solution is simple and straightforward [8], its convergence rate can be quite slow. As a result, Dawson [9] has recently published a methodology which is reported to significantly accelerate the computation of the waveguide Green's function in cases where the series expansion is "poorly" convergent [9].

In the sections which follow, a description of Dawson's algorithm, which has recently been incorporated into the AVAST code, is provided. This is followed by an illustrative example which will demonstrate the utility of this new technique.

5.2 Green's Function Acceleration

Dawson [9] has shown that the Green's function for the homogeneous waveguide case (constant fluid sound speed and density) may be expressed in the following forms,

$$G_1 = \frac{S(u,v_-;0) - S(u,v_+;0)}{4\pi H} \tag{5.1}$$

for Free-Free waveguide boundaries

$$G_2 = \frac{S(u,v_-;1/2) - S(u,v_+;1/2)}{4\pi H} \tag{5.2}$$

for Free-Rigid waveguide boundaries

$$G_3 = \frac{S(u,v_-;1/2) - S(u,v_+;1/2)}{4\pi H} \tag{5.3}$$

for Rigid-Free waveguide boundaries

$$G_4 = \frac{S(u,v_-;0) - S(u,v_+;0)}{4\pi H} \tag{5.4}$$

for Rigid-Rigid waveguide boundaries

where u and v are dimensionless variables defined as,

$$u = \frac{r\pi}{H} \tag{5.5}$$

$$v_\pm = (z \pm z')\frac{\pi}{H} \tag{5.6}$$

H is the waveguide depth, z and z′ represent the z-coordinates (height above the waveguide floor) of the source and field points, respectively, r is the distance between the field and source points measured in the x-y plane, and $S(u,v,\epsilon)$ can be expressed as a sum of images,

$$S(u,v;\epsilon) = \frac{e^{-iH\omega\left(\sqrt{u^2+v^2}\right)/c\pi}}{\sqrt{u^2+v^2}} + T(u,v;\epsilon) + T(u,-v;\epsilon) \tag{5.7}$$

where ω represents the angular frequency, c represents the fluid sound speed and $T(u,v;\epsilon)$ represents the half range sums of the form,

$$T(u,v;\epsilon) = \sum_{m=1}^{\infty} \left(e^{2\pi i\epsilon m}\right) \frac{e^{i\frac{H\omega}{c\pi}\sqrt{u^2+v^2}}}{\sqrt{u^2+(v-2\pi m)^2}} \tag{5.8}$$

It has been reported in the literature [9] that non-singular part of the Green's function found in Equations (5.1) through (5.4) is poorly convergent when the location of the field point is relatively close to the source point. However, Dawson has found that the half range sums, provided above in Equation (5.8), are amenable to convergence acceleration and can be rewritten as,

$$T(u,v;\epsilon) = \sum_{m=1}^{\infty} e^{2\pi i\epsilon m + ik(2\pi m - v)}\, Y_m(u,v) \tag{5.9}$$

where

$$k = \frac{H\omega}{c\pi} \tag{5.10}$$

and

$$Y_m(u,v) \equiv \frac{e^{-ik\left(\sqrt{u^2+(2\pi m-v)^2}-(2\pi m-v)\right)}}{\sqrt{u^2+(2\pi m-v)^2}} \tag{5.11}$$

The function $Y_m(u,v)$ can also be expressed in terms of the following expansion,

$$Y_m(u,v) \sim \frac{A_1(u,v)}{m} + \frac{A_2(u,v)}{m^2} + \frac{A_3(u,v)}{m^3} + 0\left(m^{-4}\right) \tag{5.12}$$

where the coefficients A_1, A_2 and A_3 have the following forms,

$$A_1 = \frac{1}{2\pi} \tag{5.13}$$

$$A_2 = \frac{(v - iku^2/2)}{4\pi^2} \tag{5.14}$$

$$A_3 = \frac{(v^2 - u^2(4 + 8ikv - k^2u^2)/8)}{8\pi^3} \tag{5.15}$$

Dawson then defined the following expression,

$$Y_m^*(u,v) = \frac{A_1(u,v)}{m} + \frac{A_2(u,v)}{m^2-1} + \frac{A_3(u,v)}{m(m^2-1)} \tag{5.16}$$

which he then combined with Equation (5.12), generating the following formula for $T(u,v;\epsilon)$

$$T(u,v;\epsilon) = e^{ikv}\left[Y_1X + T^*(u,v;\epsilon) + \sum_{m=2}^{\infty}\left(Y_m - Y_m^*\right)X^m\right] \tag{5.17}$$

where

$$X = e^{-2\pi i(k-\epsilon)} \tag{5.18}$$

and the function $T^*(u,v;\epsilon)$ is defined by the sum

$$T^*(u,v;\epsilon) = \sum_{m=2}^{\infty} Y_m^* X^m \tag{5.19}$$

and can be evaluated analytically. The coefficients Y_m^* (see Equation 5.16) admit a partial fraction expansion of the form

$$Y_m^*(u,v) \equiv \frac{A_1(u,v) - A_3(u,v)}{m} + \frac{A_2(u,v) + A_3(u,v)}{2(m-1)} + \frac{A_3(u,v) - A_2(u,v)}{2(m+1)} \qquad (5.20)$$

and the evaluation of the sum T^* then follows from the elementary series

$$\sum_{m+2}^{\infty} \frac{X^m}{m} = -X - \log(1-X) \qquad (5.21)$$

$$\sum_{m+2}^{\infty} \frac{X^m}{(m-1)} = -X\log(1-X) \qquad (5.22)$$

$$\sum_{m+2}^{\infty} \frac{X^m}{(m+1)} = -\frac{X}{2} + 1 - \frac{\log(1-X)}{X} \qquad (5.23)$$

5.3 Incorporation of Green's Function Convergence Acceleration Into the AVAST Code

The convergence acceleration techniques proposed by Dawson, and described in Section 5.2, have now been incorporated into an upgraded version of the AVAST code. The significant improvement in convergence performance can be judged qualitatively by considering the data presented in Figure 5.1, where Green's function estimates are plotted against the corresponding number of terms used in the series formulation. It is clear from the figure that the accelerated technique converges much more rapidly than does the original formulation and hence, representing a significant potential saving in computational time.

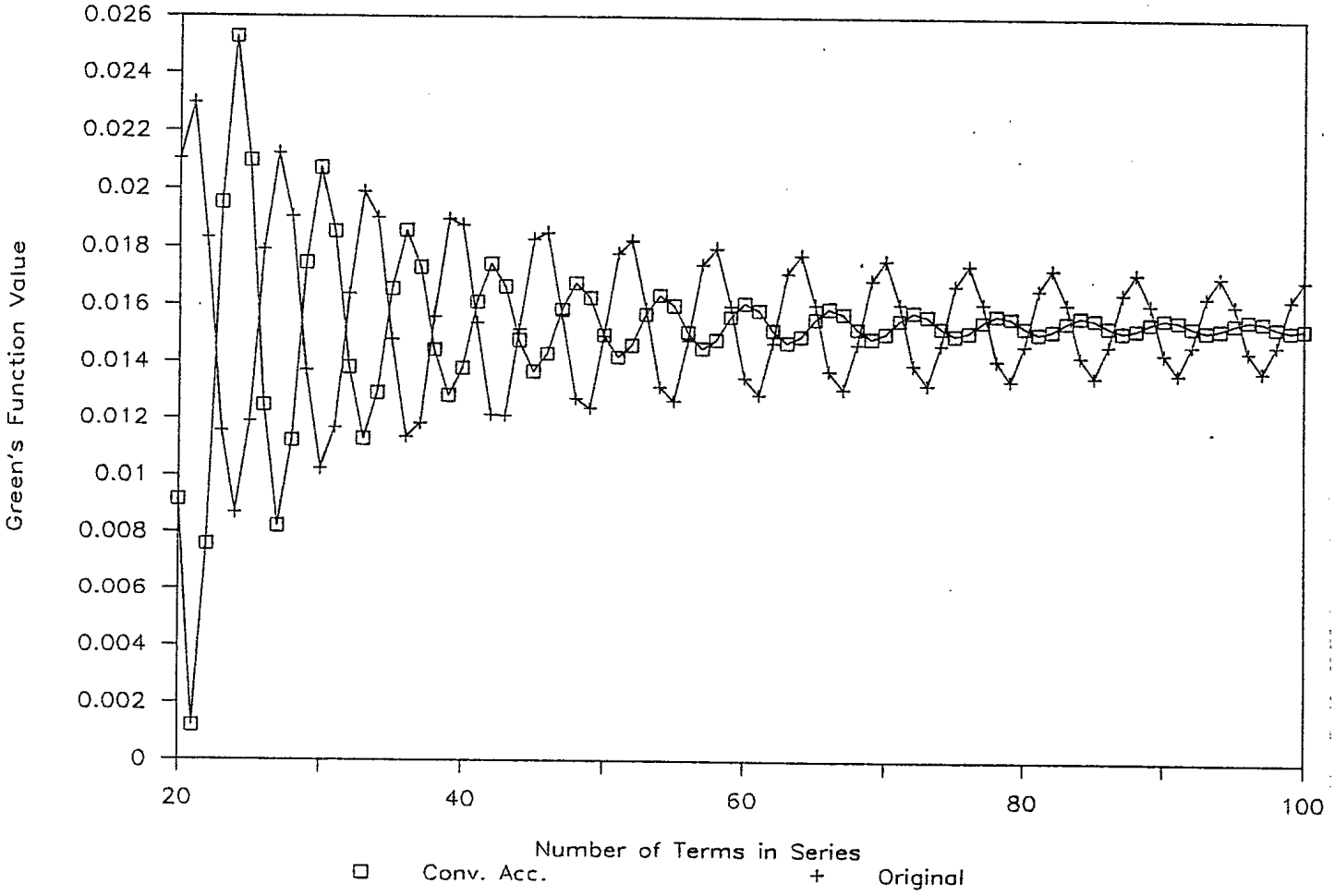

FIGURE 5.1: Convergence Acceleration Performance

6. FREQUENCY INTERPOLATION

6.1 Introduction

Cost-effectiveness of numerical schemes is a primary consideration in the development of any computational algorithm, since it determines both the economics of computation and the limit of problem solving capabilities [11]. For those researchers involved in the modelling of time harmonic acoustic radiation and scattering, both the finite element and boundary element methods have been adopted as the techniques of choice for handling large-scale problems [12]. The boundary element method (BEM) has long been a very powerful numerical technique for acoustical analysis, especially for exterior acoustic radiation and scattering. The major advantage of the BEM over other numerical methods is that only the surface of the radiating or scattering body has to be discretized (the Sommerfeld boundary condition is automatically satisfied). However, one potential shortcoming of the BEM in acoustics is that, unlike the stiffness and mass matrices generated by the finite element method, the BEM coefficient matrices are frequency dependent. Consequently, for each different frequency a new coefficient matrix must be regenerated [11]. This reformulation can be extremely expensive due to the significant numerical integration involved in setting up the matrix equations.

In an attempt to reduce computation times for multiple frequency analyses, Benthien and Schenck [11] have introduced a so-called "frequency interpolation technique." The strength of the method lies in its ability to neutralize, or smooth out, the rapidly varying Green's function found in the integral equations. Linear interpolation of the neutralized coefficient matrices between two reasonably spaced "key" frequencies can then be performed in the frequency domain.

In the sections which follow, a description of the Benthien-Schenck frequency interpolation algorithm, which has recently been incorporated into the AVAST code, is provided. This is followed by an illustrative example which will demonstrate the utility of this new technique.

6.2

6.2 Frequency Interpolation Algorithm

In the conventional boundary element method the governing differential equation is reformulated into a boundary integral equation defined on the boundary surface Ω

$$\phi(p) = \int_{\Omega} \left(\Psi(q,p) \frac{\partial \phi}{\partial n}(q) - \frac{\partial \Psi}{\partial n}(q,p) \phi(q) \right) d\Omega(q) \tag{6.1}$$

where p and q represent the spatial location of the field and source points respectively, n represents the surface normal found at point q on the body, ϕ represents the acoustic pressure, and Ψ represents the Green's function, which for an infinite fluid domain can be expressed as:

$$\Psi(p,q) = \frac{e^{-ikr_{pq}}}{4\pi r_{pq}} \tag{6.2}$$

where k represents the acoustic wavenumber and r_{pq} represents the distance between points p and q. A numerical solution of the integral equation provided in expression (6.1) can be achieved by discretizing the body surface into a series of two-dimensional surface panels. As a result, Equation (6.1) may be transformed into a system of linear algebraic equations,

$$[A]\{\phi\} = [B]\left\{\frac{\partial \phi}{\partial n}\right\} \tag{6.3}$$

where,

$$a_{mj}(k) = \int_{\Omega_j} \frac{\partial}{\partial n_j} \left(\frac{e^{-ikr(m,q)}}{r(m,q)} \right) ds(q) \tag{6.4}$$

and

$$b_{mj}(k) = \int_{\Omega_j} \frac{e^{-ikr(m,q)}}{r(m,q)} ds(q) \tag{6.5}$$

Examination of Equations (6.4) and (6.5) reveals that both components a_{mj} and b_{mj} involve the quantity e^{-ikr}, which varies rapidly with frequency when the exponent ikr is relatively large. This rapid variation in the integrands of a_{mj} and b_{mj} can be eliminated by factoring out the quantity $e^{-ikR_{mj}}$, where R_{mj} is the distance between centroids of panels m and j. Thus, a new set of matrices $\hat{A}$ and $\hat{B}$ may be defined as

$$\hat{a}_{mj}(k) = \int_{\Omega_j} \frac{\partial}{\partial n_j}\left(\frac{e^{-ik[r(m,q) - R_{mj}]}}{r(m,q)}\right) ds(q) \tag{6.6}$$

$$\hat{b}_{mj}(k) = \int_{\Omega_j} \frac{e^{-ik[r(m,q) - R_{mj}]}}{r(m,q)} ds(q) \tag{6.7}$$

The matrix coefficients defined above are slowly varying with frequency and are related to matrices A and B by

$$a_{mj} = e^{-ikR_{mj}}\hat{a}_{mj}(k) \tag{6.8}$$

$$b_{mj} = e^{-ikR_{mj}}\hat{b}_{mj}(k) \tag{6.9}$$

Linear interpolation of the neutralized coefficient matrices can then be performed between two reasonably spaced "key" wavenumbers (i.e. k_1 and k_2) to yield the matrices A and B at each intermediate wavenumber k

$$a_{mj}(k) = \alpha_1 \hat{a}_{mj}(k_1) + \alpha_2 \hat{a}_{mj}(k_2) \tag{6.10}$$

$$b_{mj}(k) = \alpha_1 \hat{b}_{mj}(k_1) + \alpha_2 \hat{b}_{mj}(k_2) \tag{6.11}$$

where,

$$\alpha_1 = \left(\frac{k_2 - k}{k_2 - k_1}\right) e^{-ikR_{mj}}$$

6.4

$$\alpha_2 = \left(\frac{k - k_1}{k_2 - k_1} \right) e^{-ikR_{mj}}$$

6.3 Incorporation of Frequency Interpolation into the AVAST Code

The frequency interpolation technique proposed by Benthien and Schenck has now been incorporated into an updated version of the AVAST code. In order to evaluate the performance of this new method the predicted radiated sound pressure levels generated by a uniformly pulsating spherical shell of radius 1.0 m, and computed using linear interpolation, were compared to the corresponding analytical solution found in the literature. The acoustic pressure values shown in Figure 6.1 were computed using base wavenumbers of 1.0 and 3.0 and compare very favourably with the exact solution.

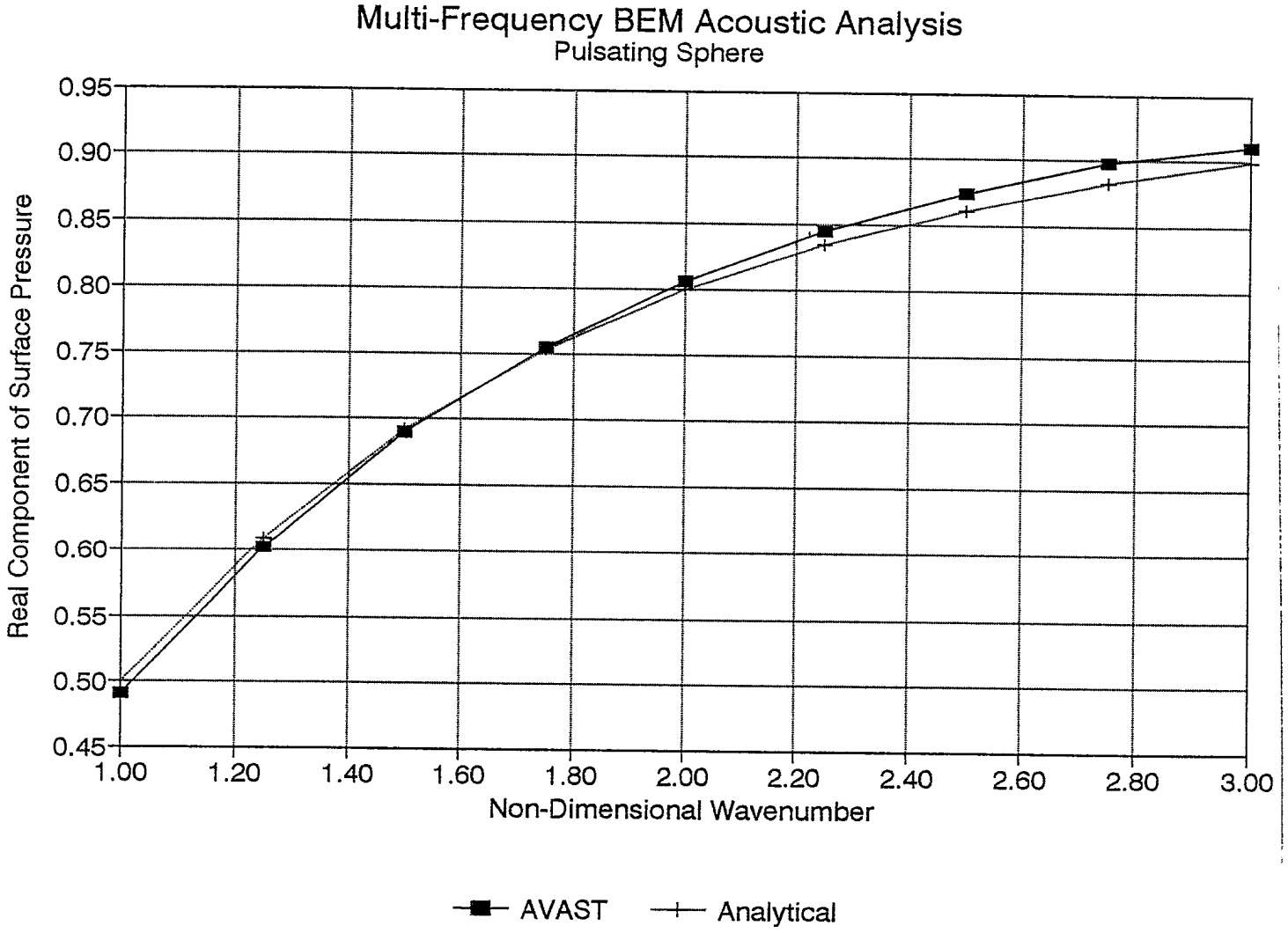

FIGURE 6.1: Acoustic Radiation Predicted using the Frequency Interpolation Technique

7. APPLICATION OF THE BURTON AND MILLAR METHOD IN AVAST

7.1 Introduction

It has been well documented in the literature that all classical integral equation formulations of the exterior Helmholtz problem fail, either through non-existence or non-uniqueness of their solutions at certain values of the acoustic wavenumber k. A comprehensive survey of the most significant approaches which have been proposed to overcome these mathematical difficulties was carried out recently by Burton [13]. In this review it was concluded that the most suitable formulation, valid for all wavenumbers, is the one originally developed by Burton and Millar [14]. The justification for this recommendation was based upon three principal criteria: reliability, numerical stability, and efficiency. A second method proposed by Schenck [15] and commonly referred to as the CHIEF method (Combined Helmholtz Integral Equation Formulation), is by far the most computationally efficient scheme available for exterior acoustic analysis, however it does not completely satisfy the reliability criterion listed above. A second major drawback of the CHIEF method is that it leads to a overdetermined system of equations. As a result, for large scale problems, use of the CHIEF method may be impractical.

Because of the above mentioned benefits of the Burton and Millar method, Martec Limited was tasked to incorporate it as an alternate to the method of Schenck in an upgraded version of the AVAST code. In the sections which follow, a brief description of the method is provided. This is followed by an illustrative example which will demonstrate the utility of this technique.

7.2 The Burton and Millar Integral Formulation

The method of Burton and Millar is based upon a linear combination of the surface Helmholtz equation,

7.2

$$\frac{1}{2}\phi(p) = \int_S \left\{ \phi(q) \frac{\partial}{\partial n_q} G(p,q) - G(p,q) \frac{\partial}{\partial n_q} \phi(q) \right\} dS(q) \qquad (7.1)$$

and its normal derivative form

$$\frac{1}{2} \frac{\partial}{\partial n_p} \phi(p) = \int_S \left\{ \phi(q) \frac{\partial^2}{\partial n_p \partial n_q} (G(p,q)) - \frac{\partial}{\partial n_p} G(p,q) \frac{\partial}{\partial n_q} \phi(q) \right\} dS(q) \qquad (7.2)$$

where,

p and q represent the acoustic field and source points respectively;
ϕ(p) represents the acoustic pressure at point p;
S represents the surface of the radiating body;
n_q represents the surface normal at point q of the body;
n_p represents the surface normal at point p of the body; and
G(p,q) represents the Green's functions appropriate for the fluid domain under consideration.

This combination leads to the following system of algebraic equations:

$$\left([A] + \beta [C] - \frac{1}{2} [I] \right) \{\phi\} = \left([B] + \beta [D] - \frac{\beta}{2} [I] \right) \left\{ \frac{\partial \phi}{\partial n} \right\} \qquad (7.3)$$

where,

$$a_{ij} = \int_{S_j} \frac{\partial}{\partial n_j} G(i,j) \, dS_j$$

$$b_{ij} = \int_{S_j} G(i,j) \, dS_j$$

$$c_{ij} = \int_{S_j} \frac{\partial^2}{\partial n_i \partial n_j} G(i,j)\ dS_j$$

$$d_{ij} = \int_{S_j} \frac{\partial}{\partial n_i} G(i,j)\ dS_j$$

[I]	represents the identity matrix
β	represents a coupling parameters (Burton and Millar suggest setting $\beta = 1/k$, where k represents the wavenumber)
S_j	represents the surface of boundary element panel j
n_j	represents the surface normal defined in panel j
n_i	represents the surface normal defined in panel i

While the uniqueness of the solutions generated by the Burton and Millar method for all wavenumbers is ensured, a highly singular kernel (due to the second derivative of the Green's function) makes numerical implementation difficult. This, according to Reut [16], was a principal reason for the method never gaining wide popularity. Fortunately, the following analytical expressions (exact for a flat rectangle or triangle surface panel s_j containing a collocation point x_j) were published in a recent article by Terai [17],

$$\int_{S_j} \frac{\partial}{\partial n_j} G(x_j, x)\, ds = 0 \qquad (7.4)$$

and

$$\int_{S_j} \frac{\partial^2}{\partial n_j \partial n_j} G(x_j, x)\, ds = -\frac{ik}{2} - \frac{1}{4\pi} \int_0^{2\pi} \frac{1}{\rho_j} e^{-ik\rho}\, d\theta_j \qquad (7.5)$$

where ρ_j represents the distance from the centroid of panel j to the panel edge. By adopting these definitions, the highly singular surface integral is converted into a non-singular contour integral, making the overall numerical implementation straight forward.

7.4

7.3 Numerical Example

The method of Burton and Millar, incorporating the analytical results published by Terai, have been implemented numerically into the AVAST code. Numerical tests have shown that for a given surface mesh the best accuracy is obtained by setting the coupling parameter β equal to i/k. In terms of an example, Figure 7.1 provides a comparison between the Burton and Millar technique, the conventional boundary integral equation formulation, and the analytical solution for the acoustic pressure generated on the surface of a uniformly pulsating spherical shell. For driving frequencies close to that of the characteristic frequency (π) the Burton and Millar formulation, in contrast to the conventional method, is able to accurately predict surface acoustic pressure levels.

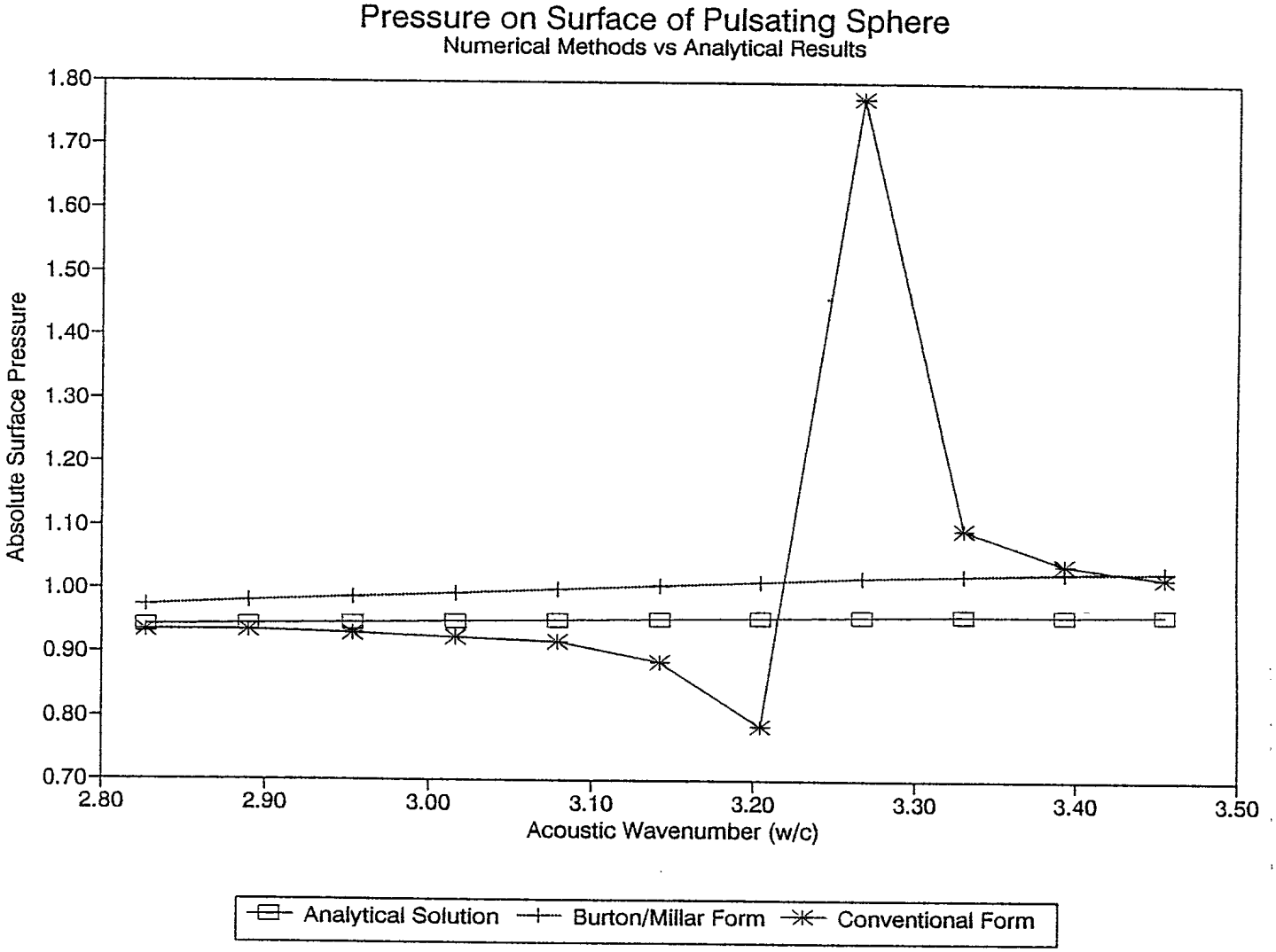

FIGURE 7.1: Performance of the Burton and Millar Method near a Characteristic Frequency

8. TRANSIENT FLUID/STRUCTURAL COUPLING

8.1 Introduction

During Phase III of the AVAST suite development work, a transient response capability was outlined and later implemented into a new version of the code. The computational method developed under this task combined a hybrid explicit and implicit time integration method based on the Kirchhoff integral Equation [18]. Compatibility of the displacements (defined by the user) along the fluid-structure interface was guaranteed by the application of the Neumann boundary condition.

Since prescribing the displacements is not practical in general, the transient acoustic fluid model described above has now been coupled with a dynamic model of an elastic structure. In the sections which follow, a review of the fluid hybrid integration method is provided. This is followed by a description of the fluid/structure coupling algorithm and the presentation of an illustrative example.

8.2 The Hybrid Time Integration Method

The acoustic radiation from a vibrating body is governed by the wave equation. The general form of the inhomogeneous scalar wave equation [19] for the pressure p at a point (r,t) is given by,

$$\Delta p(r,t) - \frac{1}{c^2}\frac{\partial^2}{\partial t^2} p(r,t) = -F(r,t) \qquad (8.1)$$

with a Newman type boundary condition relating normal structural displacements (w) to fluid pressures.

$$\frac{\partial p}{\partial n}(r,t) = -\rho \frac{\partial^2}{\partial t^2} w(r,t) \qquad (8.2)$$

where F describes a general acoustic source, n is an outward normal to the structural boundary, ρ represents the fluid density, c represents the fluid sound speed and Δ represents the Laplacian operator.

8.2

By using the time-retarded Green's function [19], $G=\delta[R/c-(t-t_0)]/4\pi R$, the pressure field p(r,t) may be described by the following integral equation,

$$C_0P(r,t) = \frac{1}{2\pi}\left[\int_S \frac{1}{R}\left(\frac{\partial P}{\partial n}\right)_{t_{ret}} dS + \int_S \frac{1}{R^2}\frac{\partial R}{\partial n}P_{t_{ret}} dS + \int_S \frac{1}{cR}\frac{\partial R}{\partial n}\left(\frac{\partial P}{\partial t}\right)_{t_{ret}} dS + \int_\Omega \frac{F(r,t-R/c)}{R} d\Omega\right] + \frac{2}{c^2}\int_S \left(G\frac{\partial P}{\partial t} - P\frac{\partial G}{\partial t}\right)\Big|_{t=0} d\Omega \quad (8.3)$$

where,

$$\frac{\partial R}{\partial n} = \cos\gamma, \quad \frac{\partial P}{\partial n} = -\rho\ddot{w}, \quad t_{ret} = t-R/c \quad (8.4)$$

where t_0 is the initial time and R is the distance between the field and source points with $C_0=2$ for field points outside the body, $C_0=1$ for field points on the surface of the body, and $C_0=0$ for field points inside the body. The symbol Ω represents the exterior fluid domain.

8.3 Incorporation into AVAST

In order to solve Equation (8.3), the surface S must be discretized into N three-noded planar elements small enough to ensure that the variable p and $\partial p/\partial n$ can be assumed to be spatially constant on each element but varying with time. Fortunately, models which have been developed by the AVAST pre-processors (stored on files having the extension **bem**) can be used by the new transient acoustic analysis code.

Discretization of the structural surface leads to the following form of Equation (8.3),

$$C_0 P(r_i,t_k) = \sum_{j=1}^{N} \frac{1}{2\pi}\left[\int_{s_j} \frac{1}{R_{ij}}(-\rho \ddot{w}_j)_{t_{ret}} dS_j + \int_{s_j} \frac{1}{R_{ij}^2}\cos\gamma_{ij} P_{t_{ret}} dS_j \right.$$
$$\left. + \int_{s_j} \frac{1}{CR_{ij}}\cos\gamma_{ij}\left(\frac{\partial P}{\partial t}\right)_{t_{ret}} dS_j\right] + \frac{1}{2\pi}\int_{\Omega_0} \frac{F(r_0,t-R/c)}{R} d\Omega_0 \qquad (8.5)$$
$$+ \frac{2}{c^2}\int_{\Omega_0}\left(G\frac{\partial P}{\partial t_0} - P\frac{\partial G}{\partial t_0}\right)\Bigg|_{t_0=0} d\Omega_0$$

with i describing the field point, j the source point and $R_{ij} = |r_i - r_j|$. If the source term, F, in Equation (8.5) can be represented by a Dirac delta function, i.e.,

$$F(r,t) = f(t)\delta(r - r_s) \qquad (8.6)$$

where R_s is the location of the source, then the integral source term in (8.5) may be rewritten as:

$$\frac{1}{2\pi}\int_{\Omega} \frac{F(r,t-R/c)}{R} d\Omega_0 = \frac{1}{2\pi}\frac{f(t_{R_s})}{R_s} \qquad (8.7)$$

By assuming that the body is initially at rest, the last integral term in Equation (8.5) will become zero by virtue of causality [17]. Hence the pressure fluid at element i on the surface of the body can be expressed at the k-th time step in the form given below:

$$P(r_i,t_k) = \frac{1}{2\pi}\sum_{j=1}^{N}\left[\frac{1}{R_{ij}}(-\rho\ddot{w}_j)_{t_{ret}} + \frac{1}{R_{ij}^2}\cos\gamma_{ij} P_{jt_{ret}}\right.$$
$$\left. + \frac{1}{cR_{ij}}\cos\gamma_{ij}\left(\frac{\partial P_j}{\partial t}\right)_{t_{ret}}\right] S_j + \frac{1}{2\pi}\frac{f(t_{R_s})}{R_s} \qquad (8.8)$$

8.4

8.3.1 Discretization of the Time Domain

Assuming that the time, t_{ret}, exists between t_k and t_{k-1}, then the pressure and its time derivative on element j may be approximated in the form,

$$P_{jt_{ret}} = (1 - \alpha_{ij})P_j^k + \alpha_{ij}P_j^{k-1} \tag{8.9}$$

$$\frac{\partial P_j}{\partial t}\Big|_{t_{ret}} = \frac{P_j^k - P_j^{k-1}}{\Delta t} \tag{8.10}$$

where $\alpha_{ij} = (t_k - t_{ret})/(t_k - t_{k-1})$. Thus whenever $\Delta t \geq R_{ij}/c$, the pressure at a field point on the j-th element is influenced by the pressure on element i at the k-th time step. This can be expressed mathematically as follows:

$$P(r_i,t_k) = \frac{1}{2\pi}\left[\frac{1}{R_{ij}}\left(-\rho\ddot{w}_j\right)_{t_{ret}} + \frac{1}{R_{ij}^2}\cos\gamma_{ij}\left\{(1-\alpha_{ij})P_j^k + \alpha_{ij}P_j^{k-1}\right\} + \frac{1}{cR_{ij}}\cos\gamma_{ij}\left(\frac{P_j^k - P_j^{k-1}}{\Delta t}\right)\right]S_j + \frac{1}{2\pi}\frac{f(t_{R_s})}{R_s} \tag{8.11}$$

8.4 Fluid/Structure Coupling

Compatibility of displacements along the fluid/structure interface is guaranteed by the application of the Neumann boundary condition, given in Equation (8.2), where the displacements u(t) can be found by solving the structural dynamic equation,

$$[M]\{\ddot{u}(t)\} + [C]\{\dot{u}(t)\} + [K]\{u(t)\} = \{f(t)\} \tag{8.12}$$

where [M], [C], and [K] represent the structural mass, damping, and stiffness matrices respectively, and $\{u(t)\}$, $\{\dot{u}(t)\}$, and $\{\ddot{u}(t)\}$ represent generalized structural displacements, velocities and accelerations, and $\{f(t)\}$ represents the applied load. In order to efficiently treat the structural dynamics equation

in the time domain, Equation (8.12) can be approximated numerically by adopting the Newmark-Beta method [20]. Doing so, yields an expression of the form,

$$[K_e]\{u\}^{t+\Delta t} = \{R\}^{t+\Delta t} \tag{8.13}$$

where

$$[K_e] = [K] + a_0[M] + a_1[C]$$

$$\{K_e\}^{t+\Delta t} = [L]\{p\}^{t+\Delta t} + (a_0\{u\}^t + a_2\{\dot{u}\}^t + a_3\{\ddot{u}\}^t)[M] + (a_1\{u\}^t + a_4\{\dot{u}\}^t + a_5\{\ddot{u}\}^t)[C]$$

$$\{\ddot{u}\}^{t+\Delta t} = a_0(\{u\}^{t+\Delta t} - \{u\}^t) - a_2\{\dot{u}\}^t - a_3\{\ddot{u}\}^t$$

$$\{\dot{u}\}^{t+\Delta t} = \{\dot{u}\}^t + a_6\{\ddot{u}\}^t + a_7\{\ddot{u}\}^{t+\Delta t}$$

[L] represents a transformation between fluid pressure and nodal forces.

$$a_0 = \frac{1}{\alpha \Delta t^2}$$

$$a_1 = \frac{\delta}{\alpha \Delta t}$$

$$a_2 = \frac{1}{\alpha \Delta t}$$

$$a_3 = \frac{1}{2\alpha} - 1$$

$$a_4 = \frac{\delta}{\alpha} - 1$$

$$a_5 = \frac{\Delta t}{2}\left(\frac{\delta}{\alpha} - 2\right)$$

$$a_6 = \Delta t(1 - \delta)$$

$$a_7 = \delta \Delta t$$

Δt represents the time step interval

$\alpha = 0.25$ (recommended in [20])
$\delta = 0.5$ (recommended in [20])

8.6

The step-by-step solution of the structural dynamics equation using the Newmark-Beta integration method proceeds in three distinct phases. Initially, the vectors $\{u\}$, $\{\dot{u}\}$, and $\{\ddot{u}\}$ are set equal to the initial conditions specified by the user. Following this, the user must then supply the time step size (Δt). In this second stage the program must form the effective stiffness matrix ($[K_e]$) and subsequently decompose it using LU decomposition. In the final phase of the analysis the algorithm generates the effective loading on the structure (which includes the surface acoustic pressures) at each time step and uses these to calculate an updated set of structural displacements, velocities and accelerations. The newly generated structural accelerations are then substituted into the Newmann boundary condition relationship (Equation (8.2)) and used to form an updated set of surface acoustic pressures.

8.5 Transient Acoustic Scattering Example

In order to demonstrate that the numerical methods found in AVAST yield accurate results for problems involving transient acoustic scattering, a model of a steel cylindrical shell (see Figure 8.1) immersed in sea water and subjected to an exponentially decaying explosive charge, was analyzed by AVAST and compared to a similar model analyzed using the USA code (see Table 8.1 for the model properties). While the AVAST suite uses the more rigorous "time retarded potential method", as opposed to the "doubly asymptotic approximation" employed in the USA code, very close agreement can be found when comparing the results provided in Figure 8.2.

TABLE 8.1: Model Properties	
Cylinder length	5 m
Cylinder radius	1 m
Shell thickness	0.01 m
Young's modulus	2.07×10^{11} Pa
Poisson's ratio	0.3
Shell density	7669 kg/m^3
Fluid sound speed	1500 m/s
Fluid density	1000 kg/m^3
Cylinder centroid	x = 0.0 m, y = 0.0 m, z = 0.0 m
Source location	x = 1000 m, y = 0.0 m, z = 0.0 m
Source time profile	$e^{-t/0.0019}$

8.8

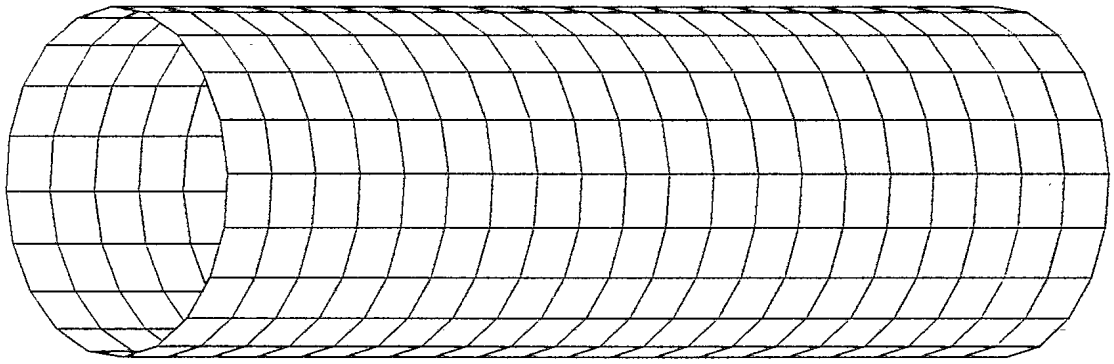

FIGURE 8.1: Discretization of Cylindrical Shell Used in the Transient Acoustic Numerical Trials

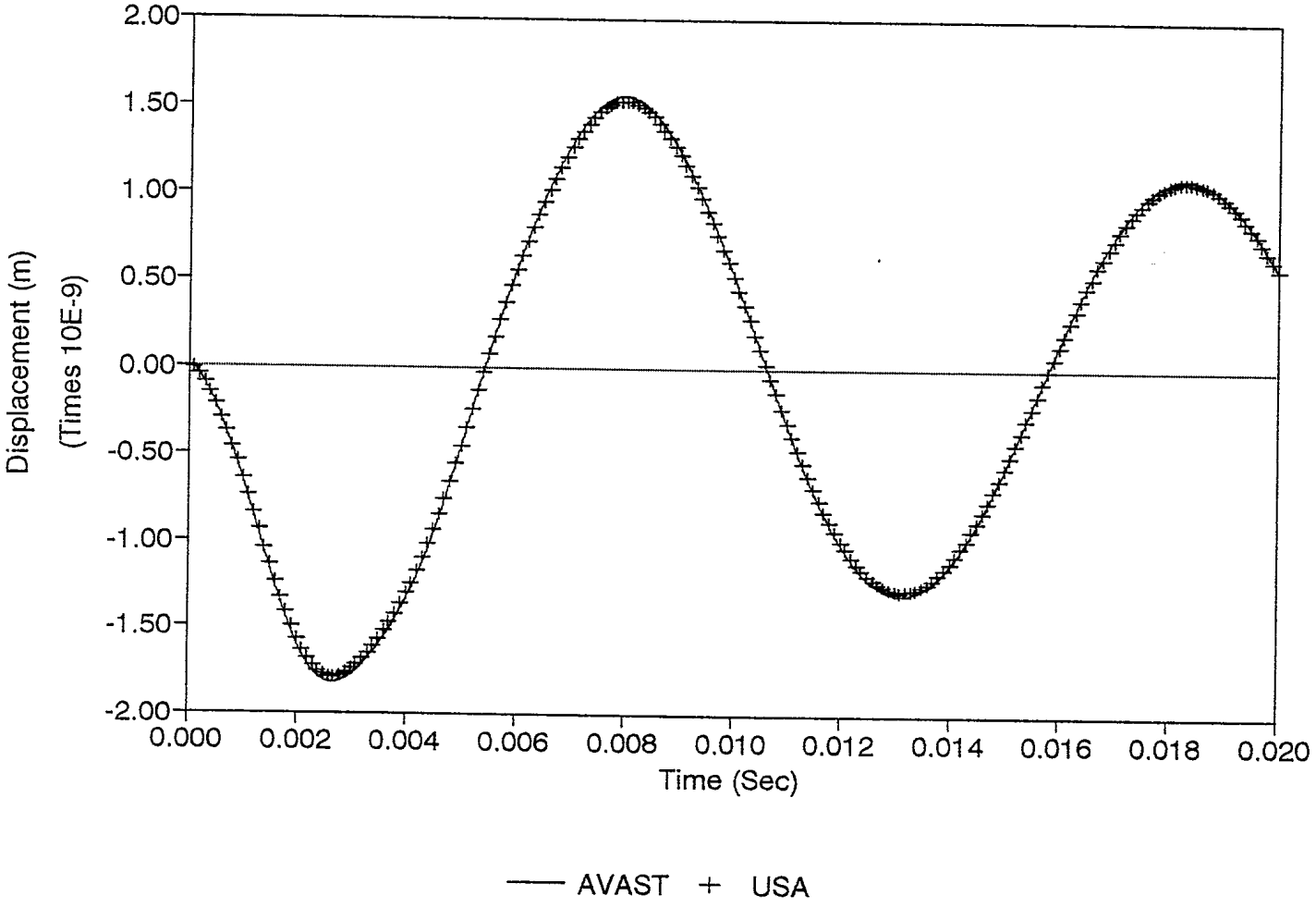

FIGURE 8.2: Radial Displacement Response of a Cylindrical Shell due to a Shock Loading Comparison of AVAST and USA Codes

9. EXPERIMENTAL/NUMERICAL EVALUATION OF PARTIALLY SUBMERGED CYLINDERS

9.1 Introduction

Defence Research Establishment Atlantic (DREA) has recently conducted experiments to measure the radiated noise from a ring-stiffened cylinder subjected to a point-driven harmonic load [21]. These tests, which were carried out at DREA Calibration Barge in Bedford Basin during the spring of 1993, have been described in full in previous DREA publications [22,23].

In the report which follows, selected data collected during these experimental trials is compared to results generated by AVAST suite of programs.

9.2 Cylinder Data

The ring-stiffened cylinder was manufactured at the Ship Repair Unit machine shops with material provided by DREA. The cylinder consists of a longitudinally welded steel tube, stiffened with ring stiffeners of square cross-section and capped with thick steel plating. The endcaps are of two pieces with a central access hatch, which is bolted to the remainder of the endcap and sealed with an O-ring. Ring bolts were welded to the endcaps at various positions to allow handling of the cylinder and the endcaps. The nominal dimensions of the cylinder are given in Table 9.1.

9.3 Numerical Modelling

A finite element model of the cylinder was provided by the Scientific Authority (see Figure 9.1). Table 9.2 provides a summary of the nodes and elements used to discretize the structure. The fluid model, describing the wet-surface or fluid/structure interface, was generated by AVAST. A plot of the boundary element fluid mesh is provided in Figure 9.2. A total of 1924 three-noded, constant pressure acoustic panels were used for this application. Fluid sound speed and density were assumed constant and were entered into the analysis as 1500 m/s and 1000 kg/m^3, respectively. It is also important to note that, due to proximity of the structure to the surface of the water, the image method,

used to model half-space fluid domains, was employed in order to account for reflections off the free surface.

9.4 Comparison of Experimental and Numerical Results

Sound pressure levels were measured at a distance of approximately 23 m from the cylinder centre, (and at a depth of 12.34 m) for the cylinder floating horizontally with half of its volume submerged. For this floating trial, the boundary element mesh used by AVAST was simply the lower half of the mesh shown in Figure 9.2.

Both AVAST and VAST/COUPLE/BEMAP codes [24,25] were used to predict the radiated noise from the floating cylinder at a frequency corresponding to the measured 2-1 mode [2]. the sound pressure level estimates calculated using these codes are compared to experimentally collected data as shown in Figure 9.3, providing excellent agreement.

TABLE 9.1: Nominal Dimensions of the Cylinder

Dimension	Value
Length	3000 mm
Diameter	762 mm
Wall thickness	9.5 mm
Endcap thickness	76.2 mm
Stiffener thickness	38.1 mm
Stiffener spacing	500 mm

TABLE 9.2: Summary of Cylinder Structural Model

Geometric nodes	962
Displacement nodes	962
Total degrees-of-freedom	5772
Shell elements	960
Beam elements	160

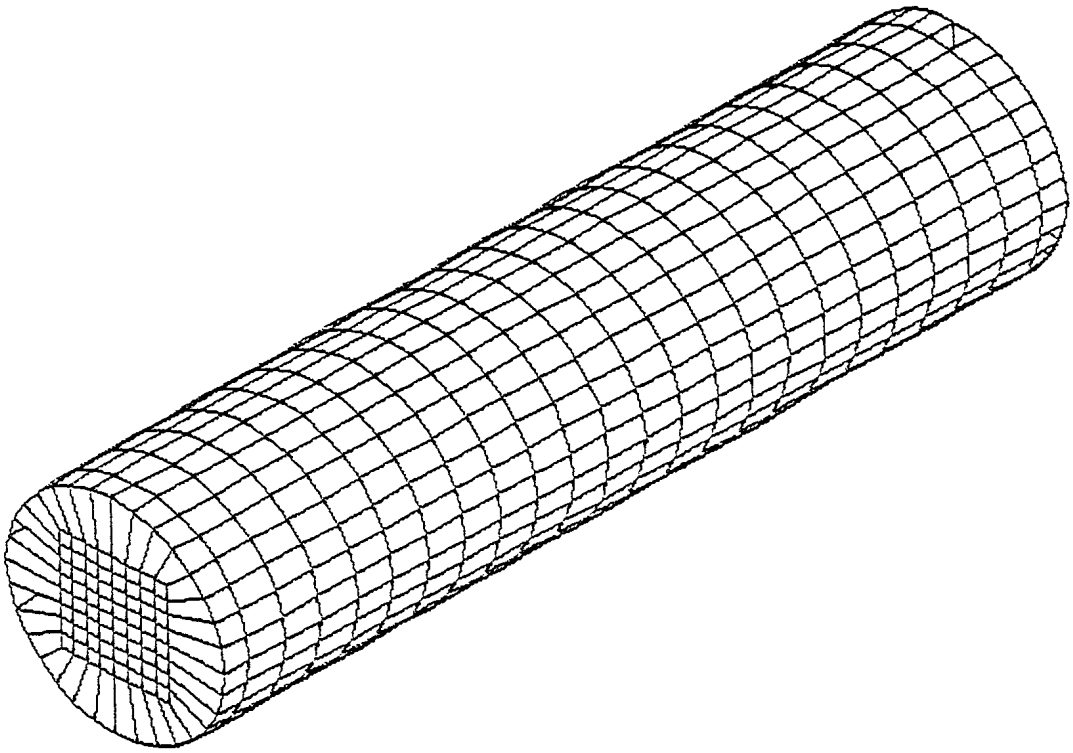

FIGURE 9.1: Exterior Surface of the Cylinder Structural Finite Element Model

9.4

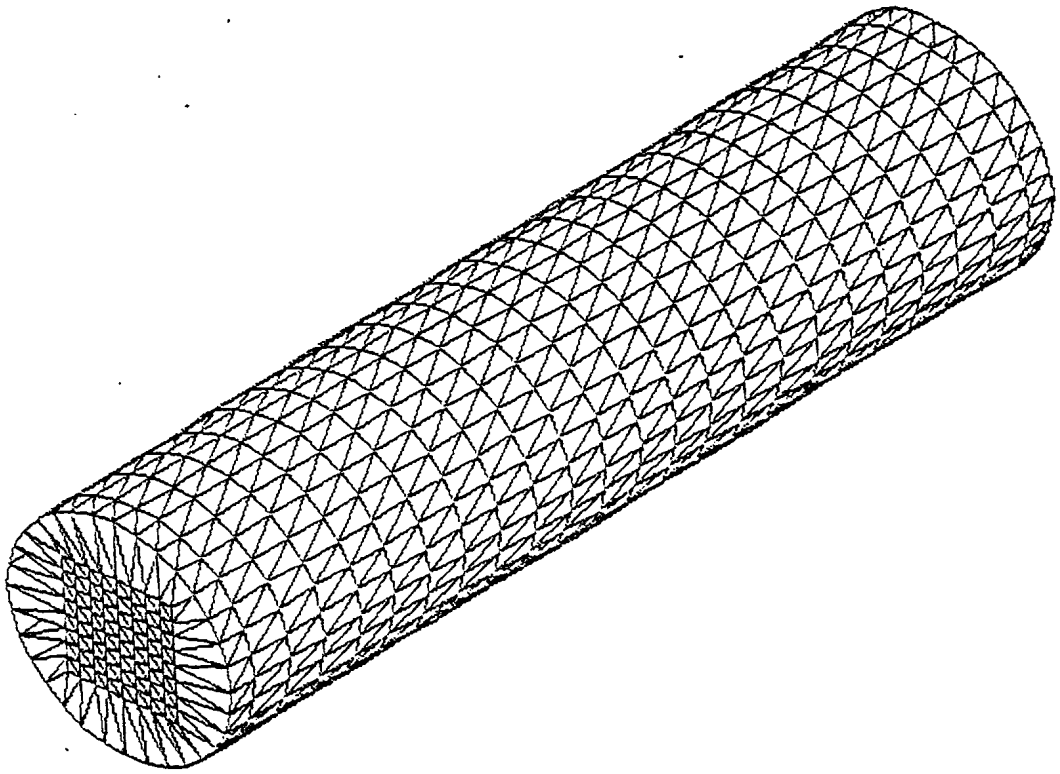

FIGURE 9.2: Boundary Element Mesh of Fluid Domain

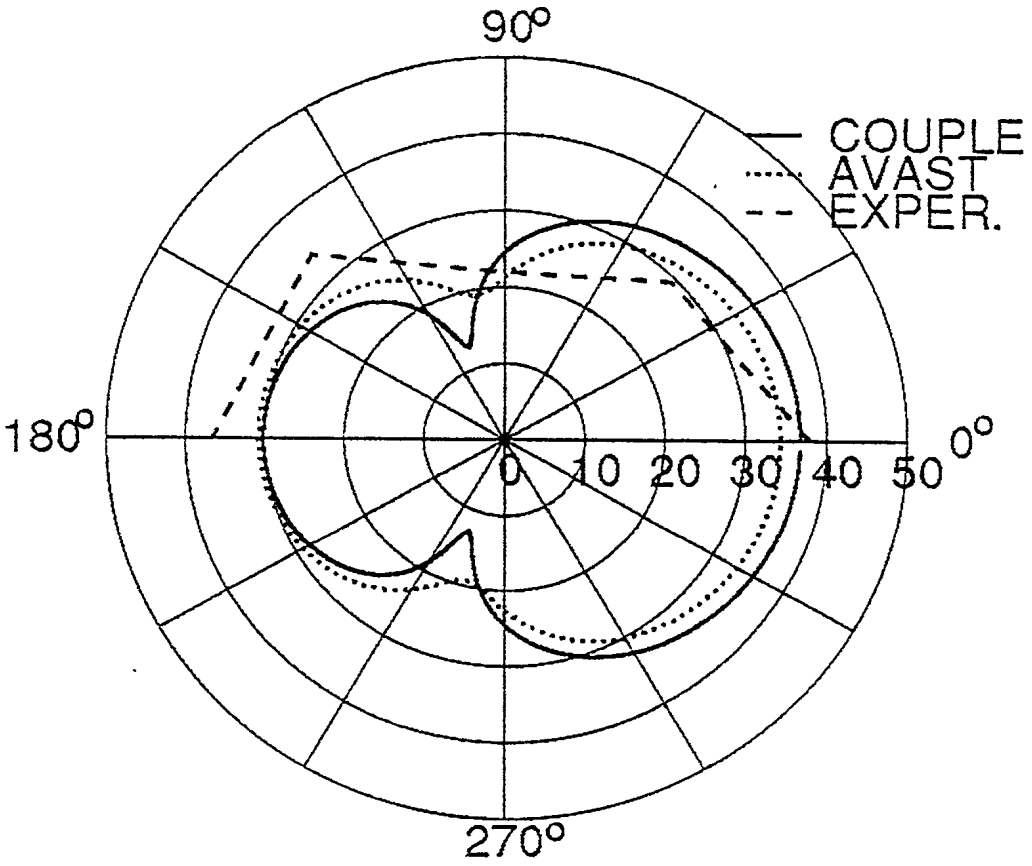

FIGURE 9.3: Directivity Pattern for Floating Cylinder

10. MODELLING RADIATED NOISE USING WET MODES

10.1 Introduction

When studying the dynamic response of structures submerged in a relatively dense fluid, the in-vacuo structural modes are often used as expansion functions for obtaining the steady state far-field pressures in the frequency domain [26]. Unfortunately, for driving frequencies below the first natural frequency of the dry structure, the in-vacuo modal approach may fail to yield acceptable results [3]. Experience has shown that when the structure is excited at frequencies corresponding to the first few "wet" natural modes of the coupled fluid/structure system (which may be significantly lower than even the first dry mode) the response generated by the in-vacuo modal method tends to be essentially static.

As a result, two separate algorithms appropriate for determining the acoustic radiation response using the wet modes of the coupled fluid/structure system have now been incorporated into the latest version of the AVAST suite. The first approach is based on a report published by Ettouney [26] and uses expansion vectors which are the vector components of the spatial part of free harmonic vibration at the forcing frequency of the fluid-structure system. In the second approach the fluid surrounding the structure is assumed to behave as a hydrodynamic fluid added mass.

In the sections which follow, a description of both wet mode approaches is provided. This is followed by an illustrative example which will demonstrate the relative effectiveness of the wet mode techniques at frequencies close to submerged natural frequencies.

10.2 Ettouney's Wet Mode Approach

The governing equation of the coupled fluid/structure system may be written as,

$$[K_s]\{\delta\} = \{F_e\} + \{F_f\} \qquad (10.1)$$

where,

$[K_s]$ represents the complex (frequency dependent) dynamic impedance matrix of the structure in-vacuo

$\{\delta\}$ represents the structural displacements normal to the wet surface
$\{F_e\}$ denotes the structural force vector
$\{F_f\}$ represents the force vector due to fluid/structure interaction

By setting $\{F_e\}$ equal to zero and noting that the fluid/structure interaction force can be obtained from the wet-surface fluid pressure $\{P\}$ by means of

$$\{F_f\} = [A]\{P\} \tag{10.2}$$

in which [A] represents the diagonal wet surface area matrix, the following equation of free vibration may be defined

$$[K_s]\{\delta\} = [A]\{P\} \tag{10.3}$$

In addition, the fluid pressure $\{P\}$ may be expressed as a series of m pressure wave mode shapes

$$\{P\} = \sum_{k=0}^{m-1} \{\phi_k\} \tag{10.4}$$

which in turn are related to a corresponding set of displacement modes through the components α_K of a diagonal modal mass matrix

$$\{\phi_K\} = -\omega^2 \alpha_K \{\xi_K\} \tag{10.5}$$

where ω represents the system driving frequency and $\{\xi_K\}$ represents the k-th displacement mode shape.

Substitution of Equation (10.5) into Equation (10.4) yields the following expression for surface pressure

$$\{P\} = -\omega^2 \sum_{k=0}^{m-1} \alpha_K \{\xi_K\} \tag{10.6}$$

which, when inserted into Equation (10.3), yields the symmetric eigenvalue problem

$$\left([K_s] - \omega^2 \alpha_K [A]\right)\{\xi_K\} = 0 \qquad (10.7)$$

from which m eigenvectors $\{\xi_K\}$ (the wet modes) and eigenvalues α_K may be obtained. It is important to note, however, that these eigenvectors and eigenvalues are unique to a specific driving frequency and as a result, a eigenvalue problem must be solved for each frequency under consideration. In addition, numerical trials have shown that the Ettouney method (as implemented in AVAST) is prone to convergence problems and as a result, has not been found to be very reliable.

10.3 Fluid Added Mass Wet Mode Approach

In order to provide an alternative to Ettouney's method, wet modes computed using the VAST code [2] may also be used to model the acoustical response of submerged structures. The computational techniques employed by VAST to generate these modes are based upon potential theory, i.e. an inviscid, incompressible fluid. In addition, it is assumed that the dominant frequency components characterizing the motion of the structure are low-frequency in nature [27] allowing the fluid effect to be modelled as a hydrodynamic added mass. This condition refers to cases in which $\lambda_{st}^2 \gg \lambda_{ac}^2$, where λ_{st} is a characteristic structural wavelength for the motion of the structural surface, $\lambda_{ac} = c/f$ is a characteristic acoustic wavelength for that motion, f represents the frequency of motion and c represents the speed of sound in the fluid.

Once these wet modes have been computed by VAST they can be used to generate the structural displacements on the wet surface. These, in turn, may then be used to calculate the sound pressure levels in the fluid.

10.4 Numerical Example

Verification of the wet-mode modelling facilities was carried out by comparing results produced by the VAST added mass approach with output generated by the conventional AVAST algorithm for a case involving the acoustic radiation produced by a point driven cylindrical arch (see Figure 10.1). Unfortunately, no meaningful results could be produced using the Ettouney algorithm. Boundary conditions were applied to the model in order to restrict the motion of the structure to the y-z plane

(see Figure 10.1). The physical properties of both the structure and the surrounding fluid are provided in Table 10.1.

The first 12 wet modes calculated by VAST were assembled for this study, the first three of these are provided in Figures 10.2 through 10.4. Figure 10.5 provides an illustration of the loads applied to the structure, which consisted of two point loads having a magnitude of 1 Newton and located at the peak of the arch. Field pressures computed for a location 1 meter directly above the arch peak, using both the wet-mode and conventional methods, is provided in Figure 10.6. It is important to note that for frequencies very close to the predicted wet natural frequency of approximately 72 Hz, the wet mode approach appears to indicate a surge in sound pressure level, while the conventional AVAST approach (described in Section 4 of this report) predicted a virtually flat response over this frequency band.

TABLE 10.1: Model Properties	
Arch Width	10 m
Arch Height	10 m
Shell Thickness	0.01 m
Young's Modulus	2.07 x 10" Pa
Shell Density	7669 Kg/m^3
Poisson's Ratio	0.3
Fluid Sound Speed	1500 m/s
Fluid Density	1000 kg/m^3

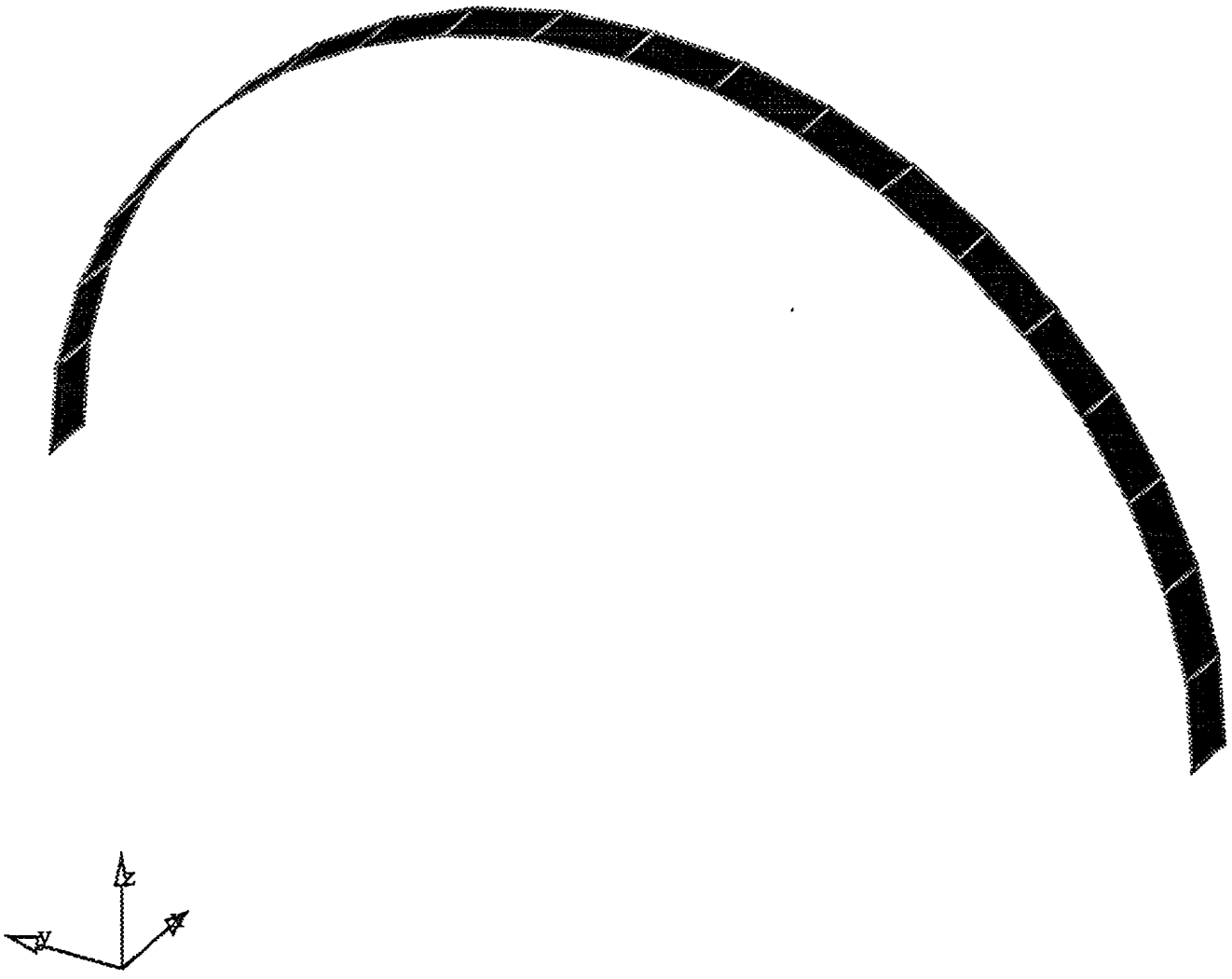

FIGURE 10.1: Finite Element Model of a Cylindrical Arch

10.6

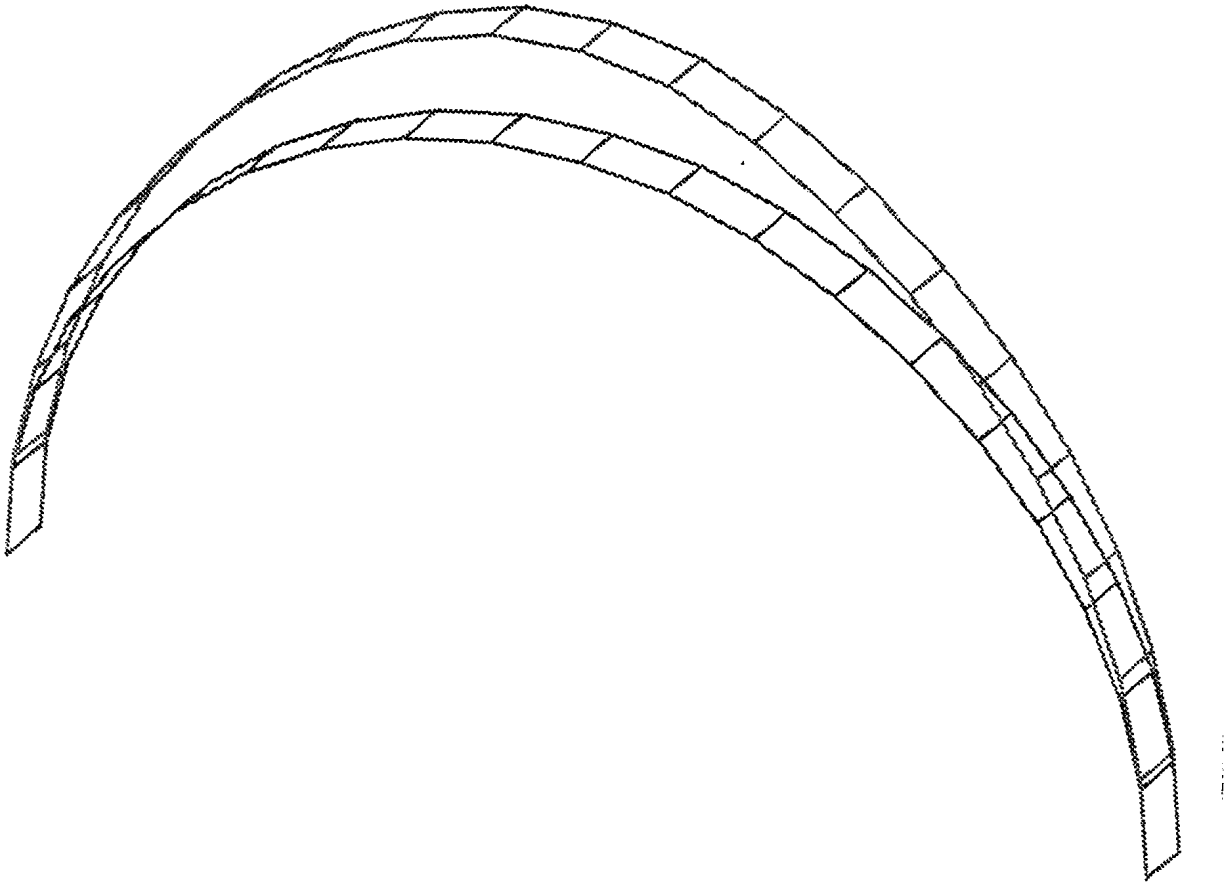

FIGURE 10.2: VAST Wet Mode Number 1

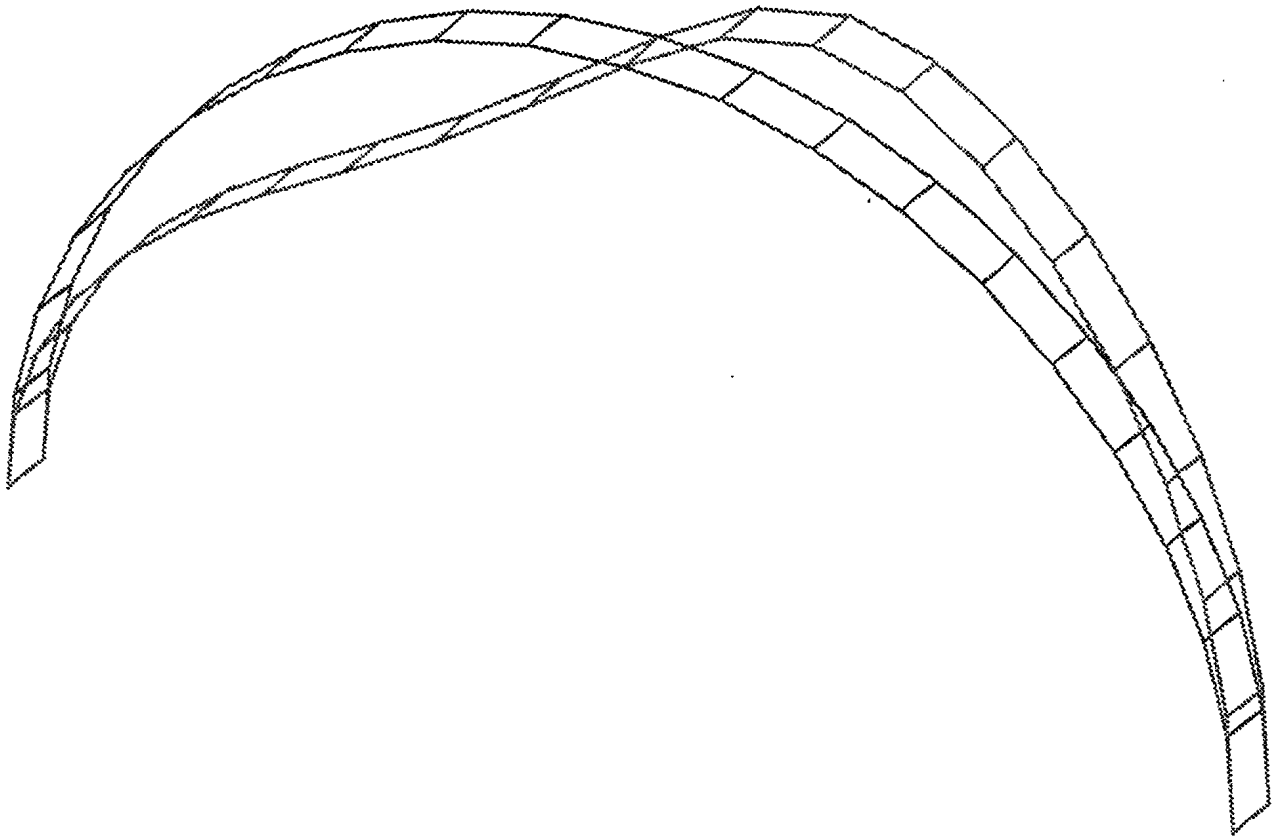

FIGURE 10.3: VAST Wet Mode Number 2

10.8

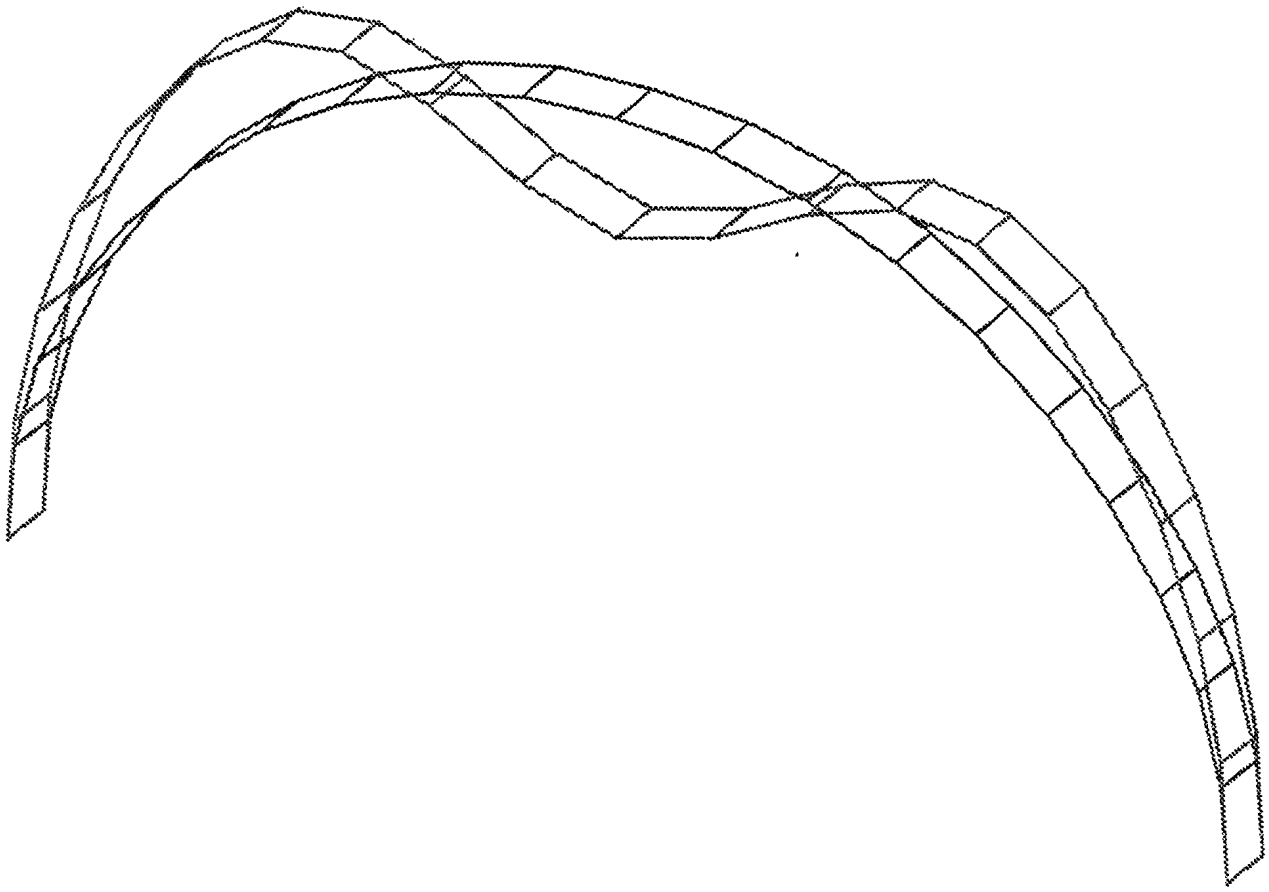

FIGURE 10:4: VAST Wet Mode Number 3

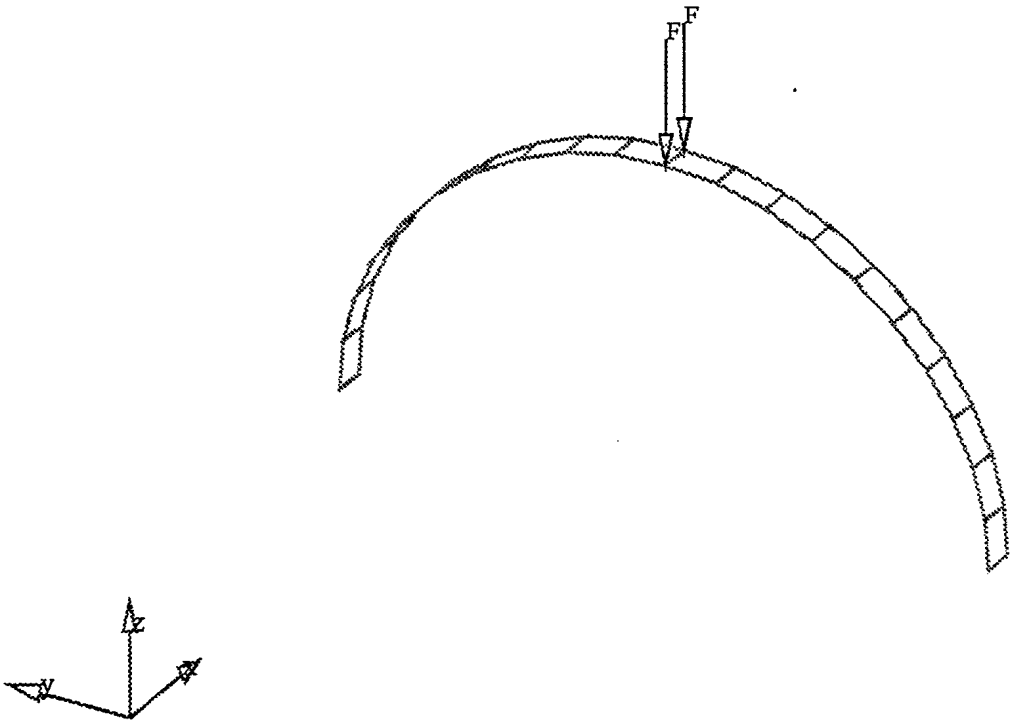

FIGURE 10:5: Structural Loading

10.10

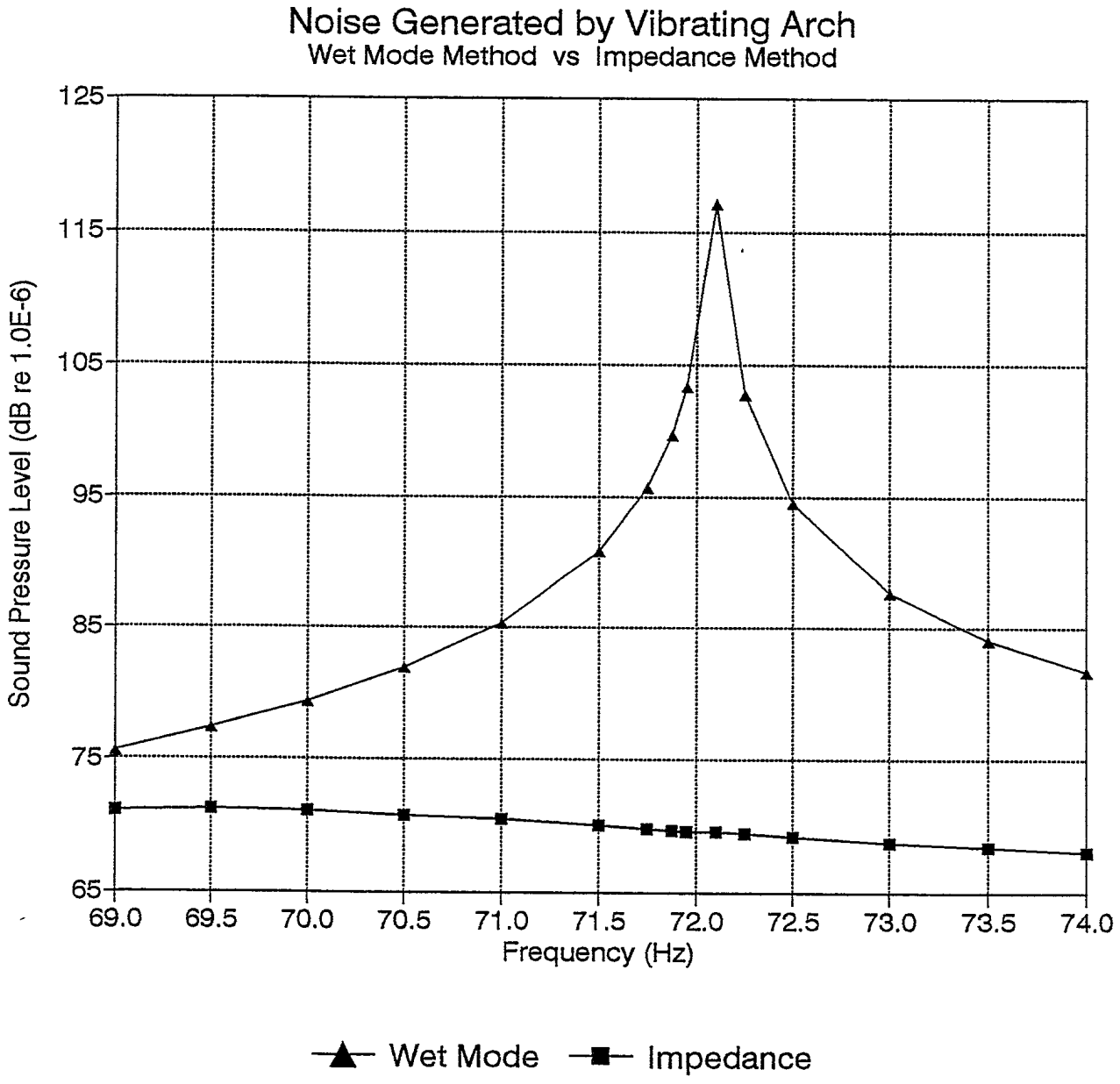

FIGURE 10:6: Noise Generated by Vibrating Arch

11. INFINITE WAVE ENVELOPE ELEMENTS

11.1 Introduction

Over the past several years, a number of numerical methods have been proposed for the modelling of acoustical wave propagation in infinite or semi-infinite fluid domains [28]. Originally domain techniques, such as the finite element and finite difference methods [29], gained considerable favour with researchers active in the field. Although obvious difficulties arise in the application of these methods to infinite domains, proponents of these techniques simply truncated the model at an arbitrary distance and applied a suitable boundary condition, such as the Sommerfeld radiation condition [30], at the distant boundary. In general, however, this lead to models of sizes which exceeded the limits of conventional computing resources, and as a result, these conventional domain techniques have been largely abandoned for more sophisticated methods.

At the present time most researchers have chosen to formulate the acoustic radiation problem in terms of an integral equation over the surface of the radiating body and solve it using the boundary element method [3]. This has the two major advantages in that the domain of interest is reduced from the three-dimensional exterior region to a two-dimensional one limited to the wet surface of the radiating body and that the Sommerfeld radiation condition is satisfied exactly. However, according to Fyfe [30], a number of disadvantages are associated with the boundary element method. From a practical point of view, one drawback is that the formulation yields fully populated, complex, nonsymmetric and frequency dependent coefficient matrices. Another well documented problem is related to the so-called non-uniqueness of the boundary element solutions at certain characteristic frequencies [1].

In light of the deficiencies with the boundary element method, considerable effort has been devoted to extend the scope of the finite element method so that it is better able to model the acoustic far field [31-35]. In one approach, a conventional finite element solution in the near field is matched to an infinite element representation in the unbounded outer region [35-37]. Because the radiation condition on the outer boundary requires the existence of outgoing waves exclusively, such that all acoustical energy is radiated outward, an appropriate asymptotic amplitude decay and wavelike

variation has been incorporated within the infinite element formulation. Although this method yields valid solutions in the inner region [36] it does not provide an accurate solution for the outer far field region.

A second approach is that of the so-called hybrid finite element/ boundary element formulation [38], whereby a conventional finite element scheme in the near field is matched with a boundary element model of the outer fluid domain. According to Astley [36], this formulation generally requires an additional degree of approximation in that the transition from the near field (finite element) to far field (boundary element) is seldom as clearly delineated as the numerical idealization requires. In addition, this method necessitates an iterative matching of impedances at the transitional interface.

More recently a new method, named the wave envelope technique [39], has been proposed in the literature. The wave envelope concept is similar in many respects to the infinite element method. Both approaches address the problem of modelling wave radiation at the outer boundary of a conventional finite element mesh surrounding a radiating body in an infinite domain. They do so by incorporating outwardly travelling, wave-like behaviour within the element shape functions. The fundamental difference between the two, however, lies in the weighting functions used in the Galerkin [20] process, which forms the theoretical basis for both methods. The case of the infinite element formulation, the weighting and shape functions are identical, yielding symmetric coefficient matrices. In the wave envelope formulation the weighting functions are complex conjugates of the shape functions. This no longer yields symmetric matrices but does eliminate the complex harmonic terms from the element integrands, providing expressions for the acoustic mass, stiffness and damping which are much simpler to evaluate.

In the report to follow a review of the latest research in the development of the wave envelope methods will be presented. Of special interest is a particular class of wave envelope element, named the infinite wave envelope element, which shows a great deal of promise in terms of complimenting the current AVAST suite.

11.2 The Wave Envelope Method

The wave envelope method originated in the study of in-duct acoustical propagation [40] but has been subsequently applied to homogeneous exterior wave problems [41] and to inhomogeneous exterior problems involving mean flow gradients [42] and temperature variations [36]. Recently, in a paper published by Astley, Macaulay and Coyette [39], the wave envelope technique was extended in two fundamental respects. First, a mapping was included in the element definition. This permitted the wave envelope region to be extended to infinity (hence the name infinite wave envelope element) and also provided greater flexibility in defining the interface between the conventional and wave envelope regions. As a rule of thumb, Astley suggested extending the inner conventional finite element mesh to a distance equivalent to approximately on acoustical wavelength with roughly seven to 10 elements per wavelength. In addition, the authors developed a modified Galerkin scheme in order to maintain the boundedness of the acoustic stiffness, mass and damping. In essence, this involved the incorporation of an additional weighting factor (equivalent to 1/r, where r approaches infinity) into the element formulation. The results produced by this modified wave envelope element were compared to both known analytical solutions and comparable boundary element studies. For simple two and three dimensional cases the wave envelope technique was found to be in excellent agreement with the analytical solutions and appeared to out-perform the boundary element method in terms of computation effort. The authors also suggested that the infinite wave envelope element method is particularly well suited to coupled acousto-structural problems with compatible, finite element, structural representations.

Cremers and Fyfe [30] have enhanced the work of Astley et al. [39] by incorporating an n-th order polynomial in the element formulation. This created the idea of a powerful element for modelling acoustic radiation. By the use of Lagrangian polynomials in the element shape functions, an arbitrary number of terms in the 1/r expansion can be generated for modelling the amplitude decay of the outgoing travelling wave. According to the authors, the implementation of this element allows for a flexible choice in the number of acoustical degrees-of-freedom in the radial infinite direction. The most significant advantage, however, is the potential for eliminating most, if not all, of the conventional finite elements modelling the acoustic near field. This may, in most cases, significantly reduce both modelling and computational times.

12. USER SUPPLIED SURFACE IMPEDANCE

The numerical evaluation of the boundary integral representation of the Helmholtz equation leads to an algebraic system of equations of the form [1],

$$[A]\{p\} = [B]\{v\} + \{P_I\} \tag{12.1}$$

where $\{p\}$ and $\{v\}$ are vectors representing the pressure and normal velocity evaluated at points located on the fluid/structure boundary, $\{P_I\}$ is a vector containing the incident pressure field values, and [A] and [B] are complex, frequency dependent, matrices.

When the surface impedance is known, an additional relationship between the pressure and velocity may be defined as [43],

$$\{p\} = -[Z]\{v\} \tag{12.2}$$

where, for local impedances [43], [Z] is a diagonal matrix whose elements relate the pressure and corresponding normal velocity within a particular surface element. Substituting equation (11.2) into (11.1) then allows for the direct solution of the surface normal velocities using the formula,

$$([B] + [A][Z])\{v\} = -\{P_I\} \tag{12.3}$$

In past versions of the AVAST suite, the impedance relationship described above could only be produced by first developing a finite element model of the structure. In order to remove this restriction, and allow for greater flexibility in the definition of surface impedances, the AVAST code has been upgraded to allow for user prescribed surface impedances. The AVAST user now has the option of providing local surface impedances (one for each fluid panel) in an ASCII file having the extension **usi**.

This data may now be extracted by the AVAST code and used to set up a system of equations similar to the form provided in Equation (12.3).

13. REFERENCES

1. D.P. Brennan and M.W. Chernuka, "Acoustic Radiation from Submerged Elastic Structures", Martec Technical Report TR-93-30, 1993.

2. "Vibration and Strength Analysis Program (VAST): User's Manual Version 7.0", Martec Ltd., Halifax, Nova Scotia, 1993.

3. S. Amini, P.J. Harris and D.T. Wilton, "Coupled Boundary Element and Finite Element Methods for the Solution of the Dynamic Fluid-Structure Interaction Problem", Springer-Verlag, New York, 1992.

4. L.E. Gilroy, Private Communication, 1993.

5. L.E. Gilroy and D.P. Brennan, "Predicting Radiated Noise From Submerged and Floating Elastic Structures", to be presented at the Third Canadian Marine Hydrodynamics and Structures Conference, Halifax, Nova Scotia, 1995.

6. G.W. Benthien and H.A. Schenck, "Structural Acoustic Coupling", in Boundary Element Methods in Acoustics (R.D. Ciskowski and C.A. Bebbia Eds.), Computational Mechanics Press, Southampton, 1991.

7. C.G. Everstine and F.M. Henderson, "Coupled Finite Element/Boundary Element Approach for Fluid-Structure Interaction", J.A.S.A., Vol. 87, No. 5, pp. 1938-1947, 1990.

8. T.W. Wu, "On Computational Aspects of the Boundary Element Method for Acoustic Radiation and Scattering in a Perfect Waveguide", J.A.S.A., Vol. 96, No. 6, pp. 3733-3743, 1994.

9. T.W. Dawson, "Acoustic Scattering in a Three-Dimensional Oceanic Waveguide Using Boundary Integral Equation Methods", J.A.S.A., Vol. 98, No. 5, pp. 2609-2622, 1991.

10. D.P. Brennan and M.W. Chernuka, "Acoustic Radiation From Submerged Elastic Structures — Phase II Report", Martec Technical Report TR-92-16, 1992.

11. T.W. Wu, W.L. LI and A.F. Seybert, "An Efficient Boundary Element Algorithm for Multi-frequency Acoustical Analysis", J.A.S.A., Vol. 94, No. 1, pp. 447-452, 1993.

12. I. Harari and T.J.R. Hughes, "A Cost Comparison of Boundary Element and Finite Element Methods for Problems of Time Harmonic Acoustics", Comp. Meth. in Appl. Mech. and Eng., Vol 97, pp 77-102, 1992.

13. A.J. Burton, "Numerical Solution of Acoustic Radiation Problems", NPL Report OC5/535, National Physical Laboratory, Teddington, Middlesex, UK.

14. A.J. Burton and G.F. Millar, "The Application of Integral Equation Methods to the Numerical Solution of Some Exterior Boundary Value Problems", Proc. Roy. Soc., Vol. A323, pp. 201-210, 1971.

15. H.A Schenck, "Improved Integral Formulations for Acoustic Radiation Problems", J.A.S.A., Vol. 44, No. 1, pp. 41-58, 1968.

16. Z. Reut, "On the Boundary Integral Methods for the Exterior Acoustic Problem", J.A.S.A., Vol. 103, No. 2, pp. 297-298, 1985.

17. T. Terai, "On the Calculation of Sound Fields Around Three-Dimensional Objects by Integral Equation Methods", J. Sound. Vib., Vol. 69, pp. 71-100, 1980.

18. D. H. Chun and T.H. Hodgson, "An Improved Computational Method for Predicting the Transient Acoustic Field from Impact Machinery", Presented at the Winter Annual Meeting of the American Society of Mechanical Engineers, San Francisco, California, 1989.

19. P.M. Pinsky and N.N. Abboud, "A Mixed Variational Principal for the Structure - Exterior Fluid Interaction Problem", in W.L. Keight (Ed.), Acoustic Phenomena and Interaction in Shear Flows Over Compliant and Vibrating Surfaces, Proc. Int. Symp. on Flow Induced Vibration and Noise, Vol. 6, ASME, 1988.

20. K. Bathe, Finite Element Procedures in Engineering Analysis, Prentice-Hall, Englewood Cliffs, New Jersey, 1982.

21. J. DeRuntz, "The Underwater Shock Code and its Applications", Presented at the 60th Shock and Vibration Symposium, Virginia Beach, Virginia, 1989.

22. L.E. Gilroy, "Natural Frequency and Radiated Noise Measurements on a Ring Stiffened Cylinder - Experimental Data Annex", DREA Technical Memorandum, December 1993.

23. L.E. Gilroy, "Proposal for a Test to Measure Acoustic Radiation from a Submerged Ring Stiffened Cylinder", DREA Technical Note, 1992.

24. L.E. Gilroy and S. Tanet, "An Improved Finite Element Based Method for Coupled Fluid/ Structure Eigenvalue Analysis", DREA Technical Memorandum 91/209, 1991.

25. A.F. Seybert and T.W. Wu, "BEMAP User's Manual - Version 2.4", Spectronics Inc., Lexington, Kentucky, 1989.

26. M.M. Ettouney, R.P. Daddazio and F.L. Dimaggio, "Wet Modes of Submerged Structures: Part I - Theory", presented at the Winter Annual Meeting of the American Society of Mechanical Engineers, Atlanta, Georgia, 1991.

27. J.A. DeRuntz and T.L. Geers, "Added Mass Computation by the Boundary Integral Method", Int. Journ. Num. Methods Eng., Vol. 12, pp. 531-549, 1978.

28. O.C. Zienkiewicz, P. Bettess, T.C. Chiam and C. Emson, "Numerical Methods for Unbounded Field Problems and a New Infinite Element Formulation", in Computational Methods for Infinite Domain Media-Structure Interaction, AMD, Vol. 46, pp. 115-147, 1981.

29. R.J. Astley and W. Eversman, "Finite Element Formulations for Acoustic Radiation", J. Sound Vib., Vol. 88, pp. 47-64, 1983.

30. L. Cremers and K.R. Fyfe, "A Variable Order Infinite Wave Envelope Element", unpublished, 1994.

31. G. Beer and J.L. Meek, "Infinite Domain Elements", Int. J. Num. Meth. Eng., Vol. 17, pp. 43-52, 1981.

32. P.P. Lynn and H.A. Hadid, "Infinite Elements with $1/r^n$ Type Decay", Int. J. Num. Meth. Eng., Vol. 17, pp. 347-355, 1981.

33. J. Marques and D.R. Owen, "Infinite Elements in Quasi-Static materially Nonlinear Problems", Comp. and Struct., Vol. 18, pp. 739-751, 1984.

34. O.C. Zienkiewicz, C. Emson and P. Bettess, "A Novel Boundary Infinite Element", Int. J. Num. Methd. Eng., Vol. 19, pp. 393-404, 1983.

35. O.C. Zienkiewicz, K. Bando, P. Bettess, C. Emson and T.C. Chiam, "Mapped Infinite Elements for Exterior Wave Problems", Int. J. Num. Meth. Eng., Vol. 21, pp. 1229-1251, 1985.

36. R.J. Astley and W. Eversman, "Wave Envelope Elements for Acoustical Radiation in Homogeneous Media", Comp. and Struct., Vol. 30, pp. 801-810, 1988

37. J.P. Goransson and C.F. Davidson, "A Three-Dimensional Infinite Element for Wave Propagation", J. Sound Vib., Vol. 115, pp. 556-559, 1987

38. S.J. Horowitz, R.K. Sigman and B.T. Zinn, "An Iterative Method for Predicting Turbofan Inlet Acoustics", AIAA, Vol. 20, pp. 1693-1700, 1982

39. R.J. Astley, G.J. Macaulay and J.P. Coyette, "Mapped Wave Envelope Elements for Acoustic Radiation and Scattering", J. Sound Vib, Vol. 170, pp. 97-118, 1994

40. K.J. Baumeister, "Finite Difference Theory for Sound Propagation in a Lined Duct with Uniform Flow Using the Wave Envelope Concept", NASA Technical Paper TP-1001, 1977

41. R.J. Astley, "Wave Envelope and Infinite Elements for Acoustic Radiation", Int. J. Numer. Meth. in Fluids, Vol. 3, pp. 507-526, 1983

42. R.J. Astley, "A Finite Element Wave Envelope Formulation for Acoustical Radiation in Moving Flows", J. Sound Vib., Vol. 103, pp. 471-485, 1986

43. A.A. Ferri, J.H. Ginsberg and P.H. Rogers, "Scattering of Plane Waves From Submerged Objects with Partially Coated Surfaces," JASA, Vol. 92, No. 3, pp. 1721-1728, 1992.

UNCLASSIFIED
SECURITY CLASSIFICATION OF FORM
(highest classification of Title, Abstract, Keywords)

DOCUMENT CONTROL DATA

(Security classification of title, body of abstract and indexing annotation must be entered when the overall document is classified)

1. ORIGINATOR (the name and address of the organization preparing the document Organizations for whom the document was prepared, e.g. Establishment sponsoring a contractor's report, or tasking agency, are entered in section 8.)

Defence Research Establishment Atlantic
P.O. Box 1012
Dartmouth, N.S. B2Y 3Z7

2. SECURITY CLASSIFICATION (overall security classification of the document including special warning terms if applicable).

UNCLASSIFIED

3. TITLE (the complete document title as indicated on the title page. Its classification should be indicated by the appropriate abbreviation (S,C,R or U) in parentheses after the title).

Enhancements of the Elasto-Acoustic Capabilities of AVAST

4. AUTHORS (Last name, first name, middle initial. If military, show rank, e.g. Doe, Maj. John E.)

Brennan, D.P.

5. DATE OF PUBLICATION (month and year of publication of document)

April 1995

6a. NO OF PAGES (total containing information Include Annexes, Appendices, etc).

61

6b. NO. OF REFS (total cited in document)

43

6. DESCRIPTIVE NOTES (the category of the document, e.g. technical report, technical note or memorandum. If appropriate, enter the type of report, e.g. interim, progress, summary, annual or final. Give the inclusive dates when a specific reporting period is covered).

Contractor Report

8. SPONSORING ACTIVITY (the name of the department project office or laboratory sponsoring the research and development. Include the address).

Defence Research Establishment Atlantic
P.O. Box 1012
Dartmouth, N.S. B2Y 3Z7

9a. PROJECT OR GRANT NO. (if appropriate, the applicable research and development project or grant number under which the document was written. Please specify whether project or grant).

Proect 1.g.1

9b. CONTRACT NO. (if appropriate, the applicable number under which the document was written).

W7707-4-2846/01-OSC

10a. ORIGINATOR'S DOCUMENT NUMBER (the official document number by which the document is identified by the originating activity. This number must be unique to this document).

DREA CR 95/461

10b. OTHER DOCUMENT NOS. (Any other numbers which may be assigned this document either by the originator or by the sponsor).

TR-95-13

11. DOCUMENT AVAILABILITY (any limitations on further dissemination of the document, other than those imposed by security classification)

(x) Unlimited distribution
( ) Distribution limited to defence departments and defence contractors; further distribution only as approved
( ) Distribution limited to defence departments and Canadian defence contractors; further distribution only as approved
( ) Distribution limited to government departments and agencies; further distribution only as approved
( ) Distribution limited to defence departments; further distribution only as approved
( ) Other (please specify):

12. DOCUMENT ANNOUNCEMENT (any limitation to the bibliographic announcement of this document. This will normally correspond to the Document Availability (11). However, where further distribution (beyond the audience specified in 11) is possible, a wider announcement audience may be selected).

Full

UNCLASSIFIED
SECURITY CLASSIFICATION OF FORM

13. ABSTRACT (a brief and factual summary of the document. It may also appear elsewhere in the body of the document itself. It is highly desirable that the abstract of classified documents be unclassified. Each paragraph of the abstract shall begin with an indication of the security classification of the information in the paragraph (unless the document itself is unclassified) represented as (S), (C), (R), or (U). It is not necessary to include here abstracts in both official languages unless the text is bilingual).

The development and incorporation of the latest enhancements to the AVAST code are described. The purpose of this work was to make the modelling of the elasto-acoustic interaction more realistic, while ensuring that the code runs as efficiently as possible. To this end, several new features have been added. These include the option to use the wet modes of the structure when generating the mobility matrix, the option to generate a structural impedance matrix based upon the mass, damping and stiffness matrices, the implementation of a multi-frequency boundary integral equation method, decomposition of the current AVAST program modules in order to allow for restart analyses, implementation of a convergence acceleration technique for use in the calculation of the waveguide Green's function, incorporation of the hypersingular Burton and Millar boundary integral equation method and the implementation of a coupling between the fluid and structural models for the transient case.

14. KEYWORDS, DESCRIPTORS or IDENTIFIERS (technically meaningful terms or short phrases that characterize a document and could be helpful in cataloguing the document. They should be selected so that no security classification is required. Identifiers, such as equipment model designation, trade name, military project code name, geographic location may also be included. If possible keywords should be selected from a published thesaurus. e.g. Thesaurus of Engineering and Scientific Terms (TEST) and that thesaurus-identified. If it not possible to select indexing terms which are Unclassified, the classification of each should be indicated as with the title).

acoustic
elasto-acoustic
numerical
finite element
boundary element
impedance
mobility
waveguide
boundary integral equation
transient
fluid-structure interaction

#154193

NO. OF COPIES NOMBRE DE COPIES	COPY NO. COPIE N°	INFORMATION SCIENTIST'S INITIALS INITIALES DE L'AGENT D'INFORMATION SCIENTIFIQUE
1	1	CML

AQUISITION ROUTE / FOURNI PAR ▶ DREA

DATE ▶ 9 NOV 91

DSIS ACCESSION NO. / NUMÉRO DSIS ▶

DND 1158 (6-87)

National Defence / Défense nationale

PLEASE RETURN THIS DOCUMENT TO THE FOLLOWING ADDRESS:

DIRECTOR
SCIENTIFIC INFORMATION SERVICES
NATIONAL DEFENCE
HEADQUARTERS
OTTAWA, ONT. - CANADA K1A 0K2

PRIÈRE DE RETOURNER CE DOCUMENT À L'ADRESSE SUIVANTE:

DIRECTEUR
SERVICES D'INFORMATION SCIENTIFIQUES
QUARTIER GÉNÉRAL
DE LA DÉFENSE NATIONALE
OTTAWA, ONT. - CANADA K1A 0K2